ISME

The Iranian Journal of Mechanical Engineering Transactions of ISME
Journal homepage: https://jmee.isme.ir/
Vol. 25, No. 2, 2024, pp. 114-141

Research Paper

DOI: https://doi.org/10.30506/jmee.2024.2023774.1341

Enrichment of Approximated Flexible Beam Model for Constrained Control of Vibration Suppression

Negin Yarinia[*]
M.Sc.

Mehdi Mirzaei[†]
Professor

Sadra Rafatnia[‡]
Assistant Professor

Masoumeh Poureshghi[§]
B.Sc. Student

For flexible beams, the application of distributed models with infinite degrees of freedom is complicated to precise control of vibration. Also, the approximated models bring uncertainties that negatively affect the controller performance. This paper aims to enhance the content of an assumed mode model of a cantilever beam by using the measurement information. A new estimation method is developed to estimate the uncertainty of the approximated model by minimizing the output estimation error at the current time. Experimentally tests are conducted to show the performance of the proposed estimation method compared with an extended state observer. Accordingly, a novel controller is developed using the estimated model to reduce the vibration of beam considering the control input limitations. The stability of the constrained second-order control system is mathematically analyzed, and its performance is evaluated through a co-simulation environment via Adams-MATLAB. The obtained results demonstrate that the suggested estimation scheme remarkably improves the accuracy of the approximated beam model. Consequently, the controller that uses the model uncertainty and disturbance information has a great efficiency in suppressing the vibrations of the beam.

Keywords: Model updating, Flexible beam, Assumed mode method, Constraint control, Vibration suppression

[*]Ph.D. Candidate, Faculty of Mechanical Engineering, Sahand University of Technology, Tabriz, Iran, ne_yarinia98@sut.ac.ir
[†]Corresponding author, Professor, Faculty of Mechanical Engineering, Sahand University of Technology, Tabriz, Iran, mirzaei@sut.ac.ir
[‡]Assistant Professor, Faculty of Mechanical Engineering, Sahand University of Technology, Tabriz, Iran, sa_rafatnia@sut.ac.ir
[§]B.Sc. Student, Faculty of Mechanical Engineering, Sahand University of Technology, Tabriz, Iran, poureshghi@gmail.com.

Received: 2024/02/26, Revised: 2024/06/13, Accepted: 2024/07/07

1 Introduction

Many advantages of flexible links, like lighter weight, higher speed, lower cost and increased power, have made them widely used in industries compared with rigid ones. However, the vibrations caused by the flexibility decrease the accuracy of devices where the flexible links are used. Therefore, the control of vibration suppression is the main challenge of flexible links[1, 2].

In order to design a precise controller for a flexible link, an accurate dynamic model with a slight complexity is required. In general, the structures have infinite degrees of freedom (DOF) because of flexibility and their mathematical models are defined by partial differential equations (PDEs). When the deflections are large, the corresponding mathematical models for the structures are nonlinear, and their complexities will be increased by taking into account the structural damping, the non-uniformity, the rotary inertia and shearing effects. Also, material and geometric uncertainties decrease the model accuracy. Despite various assumptions in developing the distributed models such as Euler–Bernoulli and Timoshenko models [3, 4], and those developed by Euler–Bernoulli theory [5-8], they remain intricate models for application in the control system design.

Since, the mathematical models defined by nonlinear PDEs are complicated to solve, some approximation techniques are presented to discretize these continuous models. The assumed modes method (AMM) [9], the lumped parameter method (LPM) [10], and the finite element method (FEM) [11, 12] are extensively utilized to approximate the continuous models of structures. Mishra and Singh [13] presented the effect of flexibility on a dynamic link model using the AMM approach, contrasting it with experimental outcomes. A comparison between two approximated models of AMM and FEM has been investigated by Tokhi and Azad [14] on a two-link flexible manipulator setup. Two discretization methods of AMM and FEM are used to simulate a rotating beam [15]. A rotating cantilever beam is modelled by the AMM in [16]. To compensate for the uncertainties of AMM-based model, a robust controller is designed for a flexible manipulator [17]. In the other paper, the controller of a two-link flexible arm manipulator is designed based on the AMM model [18]. In [19], the sliding mode controller is applied to a single-link FRM. Despite the simplicity of the approximated models for the flexible structure with a finite DOF, they contain a lot of uncertainties. The un-modeled dynamics and other uncertainties make a considerable difference between the actual and approximated models. Therefore, the controller designed by the approximated models should be robust against uncertainties that require extensive control efforts to achieve a suitable accuracy.

In this paper, a new algorithm is introduced to improve a reduced-order AMM-based model for a cantilever beam that is flexible. In the proposed scheme, a complementary phrase is appended to the nominal AMM-based model to cope with un-modeled dynamics and other uncertainties. The output of the system is defined as the end-point position of the flexible beam. Accordingly, the complementary phrase is determined by minimizing the mismatch between the measured displacement and the calculated displacement by the improved model at the current time. A novel method is suggested to predict the current-time output of the estimated model. The suggested scheme is defined in duality with the one-step-ahead controller developed in the prevalent references [20-23]. By application of this approach, a simple nominal model includes the content of the actual beam is upgraded at any moment. The constructed model is validated by the experimental examinations and the obtained responses are compared with those of an extended state observer (ESO). The ESO has been a well-known method to estimate model uncertainties and disturbances in different applications [24, 25]. However, it can estimate the unknown dynamics with bounded estimation error. The adjustment of ESO gains and its error convergence have been considered in previous researchers [26, 27]. In the current paper, an improved algorithm of ESO is employed for the uncertainty estimation of the approximated AMM-based model and the outcomes are compared with the suggested method.

After confirming the accuracy and reliability of the updated AMM-based model, it is used to design the controller for suppressing the beam vibration. The designed controller can compensate for the perturbations because of the existing complementary phrase in the design model. However, the crucial issue is finding the feasible control signal because of the limitation of actuators in generating the control inputs. To address this problem, various input-constrained control methods have been employed in the literature. In some cases, nonlinear models are presented to model the saturation of control input in combination of the system model [28, 29]. Application of anti-windup methods joined to the primary control system is another solution to address the input saturation [30]. Also, integration of proportional derivative control method based on a dynamic compensation [31] and combination of intelligent methods with Lyapunov functions [32] are suggested as alternative methods for saturation issue of control inputs. The reviewed methods, in general, still lack clarity by considering some requirements like optimality, stability and universality. Application of calculus of variation or dynamic programming for constrained systems can provide the optimality of constrained solutions [33]. To reduce computational burden of the classical optimal approaches, some approximation schemes have been introduced according to piecewise functions [34] Haar functions [35], adaptive dynamic programming (ADP) [36], hybrid functions [37] and adaptive neural network approaches [38, 39] to approximate the control input. The model predictive control (MPC) has been introduced as an alternative modern approach to calculate the constrained control signal [40, 41] Extending MPC strategies to nonlinear systems introduces some challenges, making them unsuitable for online implementations.

Apart from proposing the model-updating, another contribution of the present study is to develop a novel optimal constrained controller to suppress the beam vibration by continuous prediction of responses of the estimated model. The control law is developed in the closed form that is easy for implementation. The constrained stability of the closed loop system will be proved, and the boundedness of responses is shown. To evaluate the designed control system along with the updating algorithm, an actual model of a flexible beam is constructed in the Adams software. By application of the estimation scheme, the 1-DOF AMM model is upgraded toward the Adams model. The results determined by the suggested method are compared with some other control methods. The main contributions of the paper can be summarized as follows:

- Online updating of approximated AMM-based model of the flexible beam by uncertainties estimation using the information of displacement sensor.
- Conducting the experimental tests to show the efficiency of the proposed model updating scheme.
- Presentation of comparative results with the extended state observer to evaluate the efficiency of the proposed model updating algorithm.
- Designing a reliable constrained controller to cope with the restriction of control force, using the updated model that adapts itself to real conditions.
- Mathematical analysis of the saturated control stability within the framework of a constrained optimization problem derived by KKT theorem.
- Presentation of comparative results with the NMPC to show the proposed controller performance in the presence of perturbations and control force constraint.

The organization of the rest of the paper is as follows: Section (2) presents the dynamic modelling of the flexible cantilever beam. The proposed control algorithm is developed in Section (3). In Section (4), the experimental evaluation of the model updating algorithm is carried out, and then the suggested control strategy is investigated through the integration of Adams and MALAB software. The paper is ended by the conclusion presented at section (5).

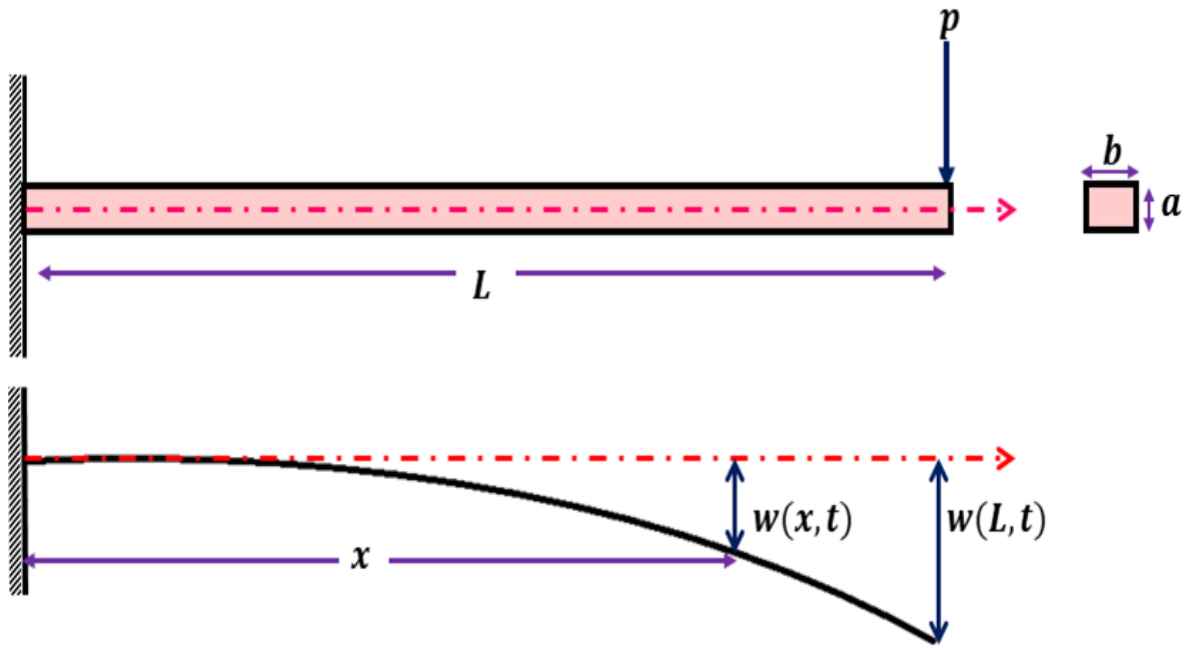

Figure 1 The diagram of the flexible beam.

2 Model of the flexible beam

Figure (1) shows a schematic of a cantilever flexible beam. The geometric characteristics including length, height and width of the beam are respectively defined by L , a and b. The beam is activated by an initial condition or a force input p at the end point.

2.1 Assumed mode model

The assumed mode method is a discretization technique used to address vibration problems in continuous systems. It tackles these problems by assuming a linear combination of admissible functions, scaled by time-dependent generalized coordinates [42]. Consequently, for a one-dimensional continuous system with one degree of freedom (1-DOF), the displacement solution is assumed to be:

$$w(x.t) = \varphi(x)\Psi(t) \tag{1}$$

in which $w(x,t)$ is the total displacement, and $\varphi(x)$ and $\Psi(t)$ are admissible function and generalized coordinate, respectively. The expressions of potential and kinetic energies are respectively defined as follow:

$$\pi(t) = \frac{1}{2}\int_0^l EI\left(\frac{\partial^2 w}{\partial x^2}\right)^2 dx \tag{2}$$

$$T(t) = \frac{1}{2}\int_0^L \rho A\left(\frac{\partial w}{\partial t}\right)^2 dx \tag{3}$$

in which $E, \rho, I,$ and a denote Young's modulus, density, area moment of inertia, and cross-sectional area of the beam, respectively. By inserting Eq. (1), into Eqs. (2), and (3), the potential and kinetic energies can be rewritten as:

$$\pi(t) = \frac{1}{2}\int_0^L EI\varphi^{"2}\,\Psi^2 dx = \frac{1}{2}\Psi^2\left(\int_0^L EI\varphi^{"2} dx\right) = \frac{1}{2}k\Psi^2 \tag{4}$$

$$T(t) = \frac{1}{2}\int_0^L \rho A\varphi^2\dot{\Psi}^2 dx = \frac{1}{2}\dot{\Psi}^2\left(\int_0^L \rho A\varphi^2 dx\right) = \frac{1}{2}m\dot{\Psi}^2 \tag{5}$$

here k and m denote the equivalent stiffness and mass of the beam, respectively:

$$k = \int_0^L EI\varphi^{"2}\,dx \tag{6}$$

$$m = \int_0^L \rho A\varphi^2\,dx \tag{7}$$

For the forced vibration problem, the virtual work of a nonconservative force is determined as follow:

$$\delta W = \int_0^L f(x,t)\delta w(x,t)dx \tag{8}$$

where $f(x,t)$ is the distributed load per unit length. By using Eq. (1), the virtual work in (8), is rewritten as:

$$\delta W = \int_0^L f(x,t)\varphi(x)\delta\Psi(t)dx = Q(t)\delta\Psi(t) \tag{9}$$

in which Q is the generalized nonconservative force. According to Fig. (1), because the point force is acting on the beam, the distributed load in Eq. (9), is replaced with $f(x,t) = p\delta(x - L)$, where p is the point force. Thus, $Q(t)$ can determined as:

$$Q(t) = \int_0^L p\delta(x-L)\varphi(x)dx = p\varphi(L) \tag{10}$$

Consequently, to present the dynamic of the system, the Lagrange equation is used as:

$$\frac{d}{dt}\left(\frac{\partial T}{\partial\dot{\Psi}}\right) - \frac{\partial T}{\partial\Psi} + \frac{\partial\pi}{\partial\Psi} = Q \tag{11}$$

By defining $q(t) = w(L,t) = \psi(t)\varphi(L)$ and substituting Eqs. (4), (5), and (10) into Eq. (11), the equation of motion of the discretized system is derived as:

$$m\ddot{q} + kq = Q\varphi(L) \tag{12}$$

By choosing the admissible function as $\varphi(x) = \frac{1}{2}\left[3\left(\frac{x}{L}\right)^2 - \left(\frac{x}{L}\right)^3\right]$ in which $\varphi(L) = 1$ the stiffness, mass and generalized nonconservative force are calculated through Eqs. (6), to (11), as:

$$k = 3\frac{EI}{L^3}, \qquad m = \frac{33}{140}\rho AL, \qquad Q = p \tag{13}$$

Equation (12) defines 1-DOF assumed mode model. Despite the simplicity of this model, it includes different sources of uncertainties due to its difference with the model of actual beam. By presenting the state space form of this model, the upgrading scheme improves its information by utilizing the sensor outputs, which measure the displacement of the end-point of the beam.

By considering $x_{1=q}$ and $x_2 = \dot{q}$ as the state variables, the state space form of equations is derived as:

$$\begin{aligned} \dot{x}_1 &= x_2 \\ \dot{x}_2 &= \frac{1}{m}p - \omega^2 x_1 \end{aligned} \tag{14}$$

where $\omega = \sqrt{\frac{k}{m}}$.

The second-order model (14), defines a reduced-order model for the actual flexible beam that have infinite degrees of freedom. By taking $\Delta(x_1, x_2, u)$ as the un-modeled dynamics, the second-order actual beam model is considered as:

$$\begin{aligned} \dot{x}_1 &= x_2 \\ \dot{x}_2 &= \frac{1}{m}p - \omega^2 x_1 + \Delta(x_1, x_2, u) \end{aligned} \tag{15}$$

4.2 Uncertainty estimation algorithms

In the following, a new algorithm is developed to estimate the uncertainty $\Delta(x_1, x_2, u)$. The proposed scheme aims to minimize the discrepancy between the sensor readings and the estimated outputs. An extended state observer as a well-known method for uncertainty estimation is also developed. These two algorithms are implemented for the flexible problem and compared.

2.2.1 Proposed estimation scheme

The improved model is developed by incorporating the complementary phrase ξ to the state space equation (14), to compensate for $\Delta(x_1, x_2, u)$ in (15) as:

$$\begin{aligned} \dot{\hat{x}}_1 &= \hat{x}_2 \\ \dot{\hat{x}}_2 &= \frac{1}{m}p - \omega^2 \hat{x}_1 + \xi \end{aligned} \tag{16}$$

The output estimated at the current instance is derived as:

$$\hat{y} = \hat{x}_1 \tag{17}$$

An optimization problem is defined to determine the complementary phrase, utilizing data obtained from the sensors. Accordingly, the following cost function is defined as:

$$J_1 = \frac{1}{2}(y - \hat{y})^2 \tag{18}$$

where the actual output y is measured by the displacement sensor. A predictive approach with one-step-aback is employed for computing the complementary phrase at the current time. This method involves deriving the estimation of $\hat{y}$ from the preceding output through the utilization of Taylor series expansion.

$$\hat{y} = \hat{y}^- + \tau\dot{\hat{y}}^- + \frac{\tau^2}{2!}\ddot{\hat{y}}^- + \cdots + \frac{\tau^k}{k!}\hat{y}^{-(k)} \tag{19}$$

where τ defines the sampling time. The sign "-" above $\hat{y}^-$ indicates the previous value, $\hat{y}^- = \hat{y}(t-\tau)$ the number of sentences in the Taylor series is selected as

$$k = a + \lambda \tag{20}$$

in which a indicates the relative of $\hat{y}$ and λ denotes the order of the estimation.

Definition 1. The lowest derivative of $\hat{y}$ for which ξ first comes into view, denotes its relative degree.

Definition 2. $\boldsymbol{\lambda}$ is defined as the estimation order if $\forall\bar{\eta}, \quad -\tau \le \bar{\eta} \le 0$

$$\xi^{[s]}(t + \bar{\eta}) \neq 0 \quad \text{if} \quad s \le \lambda$$
$$\xi^{[s]}(t + \bar{\eta}) = 0 \quad \text{if} \quad s > \lambda$$

s shows the order of the derivative.

Remark 1. The order of estimation is an important design parameter that balances the accuracy and computing efforts. By adopting zero order of estimation, ξ will be constant during the forecast period ($\xi = \xi^-$). This selection gives a fast and proper estimation for the output having low relative degrees [43, 44]**.**

As ξ explicitly appears in $\ddot{\hat{y}}^-$, the estimated output is calculated according to Eq. (19) as:

$$\hat{y} = \hat{y}^- + \tau\dot{\hat{y}}^- + \frac{\tau^2}{2!}\ddot{\hat{y}}^- \tag{21}$$

Using Eq. (16), the above equation is reformed as:

$$\hat{y} = \hat{x}_1^- + \tau\hat{x}_2^- + \frac{\tau^2}{2!}\left(\frac{1}{m}p^- - \omega^2\hat{x}_1^- + \xi\right) \tag{22}$$

After applying Eq. (22), into Eq. (18), the complementary phrase is achieved through minimization of the cost function as:

$$\frac{\partial J_1}{\partial \xi} = 0 \tag{23}$$

Solution of Eq. (23), gives:

$$\xi = -\frac{2}{\tau^2}\left[\hat{x}_1^- - x_1 + \tau\hat{x}_2^- + \frac{\tau^2}{2}\left(\frac{1}{m}p^- - \omega^2\hat{x}_1^-\right)\right] \tag{24}$$

The estimation error is derived by substituting (24), into (22), as:

$$y = \hat{y} \tag{25}$$

According to (25), the enhanced AMM-based model accurately follows the behavior of actual system, resulting in zero estimation error. Note that, in practice, the measurement noise and consequently the estimation error is stochastic and can be attenuated by a low-pass filter. Therefore, the complementary phrase ξ in the estimated model (16), successfully compensates for the uncertainty term Δ in (15).

2.2.2 ESO algorithm

In the ESO scheme, the perturbation term is determined as an extra state $x_3 = f(x) = -\omega^2 x_1 + \Delta(x_1, x_2, u)$. Then, the expanded state space form of the AMM-based model is articulated as:

$$\begin{aligned} \dot{x}_1 &= x_2 \\ \dot{x}_2 &= x_3 + \frac{1}{m}p \end{aligned} \tag{26}$$

$$\begin{aligned} \dot{x}_3 &= \Upsilon(t) \\ y &= x_1 \end{aligned} \tag{27}$$

where $\Upsilon(t) = \dot{f}(x)$ is suppose bounded. Therefore, the estimated state in the ESO algorithm is defined as:

$$\begin{aligned} \dot{\hat{x}}_1 &= \hat{x}_2 - \phi_1(\hat{x}_1 - y) \\ \dot{\hat{x}}_2 &= \hat{x}_3 + \frac{1}{m}p - \phi_2(\hat{x}_1 - y) \\ \dot{\hat{x}}_3 &= -\phi_3(\hat{x}_1 - y) \end{aligned} \tag{28}$$

in which $\phi_{i\ (i=1,2,3)}$ represents the observer coefficients. By appropriately choosing these coefficients, the ESO provides an estimation of all states, encompassing the supplementary state x_3 that incorporates model uncertainty. By subtracting equation (27) from equation (29), the dynamics of the observer error are determined as:

$$\begin{aligned} \dot{e}_1 &= e_2 - \phi_1 e_1 \\ \dot{e}_2 &= e_3 - \phi_2 e_1 \\ \dot{e}_3 &= -\Upsilon(t) - \phi_3 e_1 \end{aligned} \tag{29}$$

in which $e_i = \hat{x}_i - x_i$ $(i = 1,2,3)$ represents the estimation errors. Equation (29) shows that the dynamics of the estimation error are linear. Accordingly, by supposing the boundedness of $\Upsilon(t)$, the bounded-input, bounded-output (BIBO) stability of the estimation error can be achieved by appropriately tuning the observer coefficients. The selection of $\phi_{i\ (i=1,2,3)}$ is outlined as follows:
Theorem 1. Choosing $\phi_1 = 3/\varepsilon$, $\phi_1 = 3/\varepsilon^2$ and $\phi_3 = 1/\varepsilon^3$, where ε is a free value, the estimation error dynamics given by equation (29) remain bounded, assuming that $\Upsilon(t)$ is bounded.**Proof.** Using, $\phi_1 = 3/\varepsilon$, $\phi_1 = 3/\varepsilon^2$ and$\phi_3 = 1/\varepsilon^3$in the estimation error dynamics (29), relies on:

$$\begin{bmatrix}\dot{e}_1\\ \dot{e}_2\\ \dot{e}_3\end{bmatrix} = E\begin{bmatrix}e_1\\ e_2\\ e_3\end{bmatrix} - G\Upsilon(t) \tag{30}$$

where $E = \begin{bmatrix} -3/\varepsilon & 1 & 0\\ -3/\varepsilon^2 & 0 & 1\\ -1/\varepsilon^3 & 0 & 0\end{bmatrix}$ and $G = \begin{bmatrix}0\\0\\1\end{bmatrix}$. The three eigenvalues of E are identical to $\lambda_i = -\frac{1}{\varepsilon}$ $(i = 1,2,3)$. Consequently, for any specified $\varepsilon > 0$, the matrix E becomes Hurwitz, ensuring BIBO stability of the error dynamics. The parameter ε, which is adjustable, influences the convergence rate of estimation errors. Solving Eq. (30) with positive values for ε yields:

$$\lim_{t\to\infty} e(t) = \int_0^t e^{E(t-\tau)} G\Upsilon(\tau)d\tau \tag{31}$$

From equation (31), it is deduced that for any specified $\varepsilon > 0$, the estimation error dynamics remain bounded, assuming that $\Upsilon(t)$ is bounded [45].

Remark 2. The coefficient ε affects the speed of the extended state observer. Smaller values of this coefficient lead to quicker responses. On another hand, smaller value of the coefficient ε increases sensitivity to measurement noise and modeling errors.

3 Controller design

To attenuate the vibration of the beam, a control system is developed using the enriched AMM model (16). In the suggested control scheme, the control input is defined as the force applied at the end of the beam ($\boldsymbol{p} = \boldsymbol{u}$). In the following, at first the unconstrained control is presented in which the input constraint is dropped. Then the constrained version is developed and its stability is analyzed.

3. 1 Unconstrained control

The fundamental concept of the control method is to determine the present control input by minimization of the subsequent error. By regarding the end-point position as the system output, a cost function is formulated to penalize the forthcoming tracking error as

$$\boldsymbol{J_2} = \frac{\mathbf{1}}{\mathbf{2}}[\boldsymbol{y}(\boldsymbol{t}+\boldsymbol{h}) - \boldsymbol{y_d}(\boldsymbol{t}+\boldsymbol{h})]^{\mathbf{2}} \tag{32}$$

here $h > 0$ denotes the time of prediction. In addition, y_d indicates the reference output. The next-time responses in (32) must be determined using the Taylor series that its number of sentences is limited to the relative degree [46-48]. According to Eq. (16), the relative degree of $y = \hat{x}_1$ with respect to the control input is found to be two because the control signal is first appearing in the second derivative of the output as

$$\ddot{\hat{x}}_1 = \frac{1}{m}u - \omega^2\hat{x}_1 + \xi \tag{33}$$

Therefore, the prediction of the response and the desired one is explained as

$$y(t+h) = y(t) + h\dot{y}(t) + \frac{h^2}{2}\ddot{y}(t) \tag{34}$$

$$y_d(t+h) = y_d(t) + h\dot{y}_d(t) + \frac{h^2}{2}\ddot{y}_d(t) \tag{35}$$

Substituting Eq. (16) into (34) gives

$$y(t+h) = \hat{x}_1 + h\hat{x}_2 + \frac{h^2}{2}\left(\frac{1}{m}u - \omega^2\hat{x}_1 + \xi\right) \tag{36}$$

Assuming $y_d = x_{1d}$ and using (35) and (36), the function (32) can be rewritten as

$$J_2 = \frac{1}{2}\left[(\hat{x}_1 - x_{1d}) + h(\hat{x}_2 - \dot{x}_{1d}) + \frac{h^2}{2}\left(\frac{1}{m}u - \omega^2\hat{x}_1 + \xi - \ddot{x}_{1d}\right)\right] \tag{37}$$

Using the following optimality condition:

$$\frac{\partial J_2}{\partial u} = 0 \tag{38}$$

leads to the following control law:

$$u = -\frac{2m}{h^2}\left[(\hat{x}_1 - x_{1d}) + h(\hat{x}_2 - \dot{x}_{1d}) + \frac{h^2}{2}(-\omega^2\hat{x}_1 + \xi - \ddot{x}_{1d})\right] \tag{39}$$

By applying (39) in (33), the tracking error dynamics is derived as

$$\ddot{e} + \frac{2}{h}\dot{e} + \frac{2}{h^2}e = 0 \tag{40}$$

Remark 3. Since the prediction time h is positive, the linear regulation error dynamics (40) is exponentially stable. It is seen that the prediction time has the role of the time constant for the controlled system. The prediction time also effects the time constant of the error dynamic (40). The poles of Eq. (40), are calculated as $-\frac{1}{h}(1 \pm j)$. Therefore, the prediction time influences the place of poles and the system output. Smaller values of h result in faster responses.

3.2 Constrained control

The input constraint is a physical limitation due to the limited capacity of control actuators. Consequently, the control input must lie within the acceptable range as

$$u^{\min} \leq u \leq u^{\max} \tag{41}$$

To derive the constrained control input, the cost function (37) is minimized subject to the input constraints (41). The constrained optimization problem is solved using Kerush-Kuhn-Tucker (KKT) theorem. In this respect, the standard form of the constraint (41) is first determined as:

$$\begin{aligned} q_1 &= u - u^{\max} \le 0 \\ q_2 &= -u + u^{\min} \le 0 \end{aligned} \tag{42}$$

Then, the following optimality conditions based on the KKT theorem are stated as [49].

$$\frac{\partial J_2}{\partial u} + \sum_{i=1}^{2} \lambda_i \frac{\partial q_i}{\partial u} = 0 \tag{43}$$

$$\lambda_i q_i = 0 \quad i = 1,2 \tag{44}$$

$$q_i \le 0 \quad i = 1,2 \tag{45}$$

$$\lambda_i \ge 0 \quad i = 1,2 \tag{46}$$

where λ_1 and λ_2 indicate Lagrange multipliers.

Theorem 2. For a single input system defined by Eq. (16) with upper and lower bounds, the constrained solution will be a simple saturated version of the unconstrained controller.

Proof. To find the constrained solution, the KKT conditions (43) to (46) are required to be investigated simultaneously. According to (44) to (46), the inactivity of the constraints indicates and $q_i \le 0$ and $\lambda_i = 0$, since the Lagrange multipliers are nonzero for the active constraints ($\lambda_i = 0$) and the corresponding control inputs are straightly obtained by the constraint equations $q_i = 0$. Accordingly, the non-zero Lagrange multiplier where the constraint is inactive are determined via Eq. (44). For both inactive constraints, corresponding Lagrange multipliers will be zero, leading to the unconstrained solution. For the FB with single control input, the resulting constrained controller is defined as follows:

$$u_{\text{cons}} = \begin{cases} u^{\max} & \text{if} \quad q_1 \ge 0\,, q_2 < 0 \\ u_{\text{unc}} & \text{if} \quad q_1 \le 0\,, q_2 \le 0 \\ u^{\min} & \text{if} \quad q_1 < 0\,, q_2 \ge 0 \end{cases} \tag{47}$$

where u_{unc} is the unconstrained control input presented in (39). In order to analyze the stability of constrained solution, Eq. (43) can be rewritten using constraints (42) as:

$$\frac{\partial J_2}{\partial u} = C \tag{48}$$

in which $C = \lambda_2 - \lambda_1$. By solving (48), the constrained controller corresponding to the term, $C$is derived as:

$$u = \frac{4m^2}{h^4} C - \frac{2m}{h^2}\left[(\hat{x}_1 - x_{1d}) + h(\hat{x}_2 - \dot{x}_{1d}) + \frac{h^2}{2}(-\omega^2 \hat{x}_1 + \xi - \ddot{x}_{1d})\right] \tag{49}$$

The following analysis shows the boundedness of the beam dynamic under the control input (49). Equivalently, the boundedness of constrained solution is provided.

The dynamics of the controlled system is obtained by applying Eq. (49), in the model. (33), as:

$$\ddot{e} + \frac{2}{h}\dot{e} + \frac{2}{h^2}e = \frac{4m}{h^4}C \tag{50}$$

The right-hand side term of (50), arise from limiting the control signal via the C containing Lagrange multipliers. Due to boundedness of Lagrange multipliers, the upper bound Ω can be selected for the mC in the right-hand side of Eq. (50). Therefore, the following inequality can be derived:

$$\ddot{e} + \frac{2}{h}\dot{e} + \frac{2}{h^2}e \leq \frac{4}{h^4}\Omega \tag{51}$$

The above differential inequality can be solved using the comparison lemma [50] as:

$$e \leq Ae^{\frac{-1}{h}t}\left(\sin\frac{1}{h}t + \emptyset\right) + \frac{2\Omega}{h^2} \tag{52}$$

The positive values for h indicates that:

$$\lim_{t\to\infty} e = \frac{2\Omega}{h^2} \tag{53}$$

According to Eq. (53), for any specified $\gamma > 0$, choosing the prediction time as $h^2 > \frac{2\Omega}{\gamma}$ ensures the convergence of e to the following compact set:

$$\|e\| < \gamma \tag{54}$$

To evaluate the boundedness of $\dot{e}(t)$, a potential Lyapunov function candidate can be considered in the form of:

$$V = \frac{1}{h^2}e^2 + \frac{1}{2}\dot{e}^2 \tag{55}$$

The derivative of V leads:

$$\dot{V} = \frac{2}{h^2}e\dot{e} + \dot{e}\ddot{e} \tag{56}$$

Using Eq. (50), in Eq. (56), gives:

$$\dot{V} = -\frac{2}{h}\dot{e}^2 + \frac{4m}{h^4}C\dot{e} \tag{57}$$

that gives:

$$\dot{V} \leq -\frac{2}{h}\dot{e}^2 + |\dot{e}|\left|\frac{4m}{h^4}C\right| \tag{58}$$

The second term in the right-hand side of Eq. (58), is replaced using the inequality $\kappa\mu \leq n\kappa^2 + \frac{\mu^2}{4n}$ for any real κ, μ and $n > 0$. Defining $n = \frac{1}{h} > 0$

$$\dot{V} \leq -\frac{1}{h}|\dot{e}|^2 + \frac{4}{h^7}|mC|^2 \tag{59}$$

Considering $|mC| \leq \Omega$, gives:

$$\dot{V} \leq -\frac{1}{h}|\dot{e}|^2 + \frac{4}{h^7}\Omega^2 \tag{60}$$

Equation (60), can be obtained by using Eqs. (60), and (55), as:

$$\dot{V} \leq -\frac{2}{h}V + \frac{2}{h^3}e^2 + \frac{4}{h^7}\Omega^2 \tag{61}$$

Applying the upper bound of (54), results in:

$$\dot{V} \leq -\frac{2}{h}V + \frac{2}{h^3}\gamma^2 + \frac{4}{h^7}\Omega^2 \tag{62}$$

By taking $R = \frac{2}{h^3}\gamma^2 + \frac{4}{h^7}\Omega^2$, Eq. (62) is presented as

$$\dot{V} \leq -\frac{2}{h}V + R \tag{63}$$

The above differential inequality can be solved using the comparison lemma

$$V(t) \leq \left(V(0) - \frac{h}{2}R\right)e^{-\frac{2}{h}t} + \frac{h}{2}R \tag{64}$$

which implies that, the Lyapunov function remains bounded for any specified $h > 0$ as

$$\lim_{t\to\infty} V = \frac{h}{2}R \tag{65}$$

According to Eq. (65), the Lyapunov function is bounded. On the other hand, as shown in (54) the tracking error is within a compact set. These results guarantee the boundedness of $\dot{e}.^{+}$

Remark 4. The value of h, as a controller parameter, is tuned for improving the controller performance. It effects on the time constant and the convergence rate of the closed loop stable system. For smaller value of h, the system response will be faster at the cost of higher amount of the control input in the unconstrained control. This aligns with the outcome of Theorem 2, which indicates that h should not be smaller than a certain value to ensure the system's responses remain within limits under constraints.

4 Result and discussion

Both experimental and simulation results of this research are presented in this section. The proposed estimation method is implemented in the experimental part to evaluate its

effectiveness through the real tests of the cantilever beam. In this part, information from measurement is used to enhance the nominal AMM-based model, resulting in a more accurate representation of the real-world system. In the second part, the Adams-MATLAB co-simulation is employed to evaluate the performance of the proposed control system. Here, a predictive unconstrained and constrained controllers designed using the estimated model, are examined to reduce the vibration of the end-point displacement.

4.1 Experimental verification of the model-updating scheme

Referring to Fig. (2), a capacitor sensor is used to measure the displacement of the beam end-point. The LabVIEW software integrated with the Advantech PCI card 1716 is utilized to process the measured data. The collected data is used to u
pdate the initial assumed mode model. The algorithm verification is done by comparing the responses of the updated model with the measured data. In this collection, the forced vibrations are provided by an electrical imbalance exciter.

4.1.1 Free vibration

The beam vibration ("Case-1") with the initial end-point displacement of $1(mm)$ is considered as the free vibration. The obtained results that compare the initial and updated models are depicted in Fig. (3). Also, 20% error between the initial conditions of actual and constructed model is considered. As shown in Fig. (3a), the end-point displacement of the nominal model differs from the experimental data due to different sources of perturbations. However, according to Fig. (3c), the existing difference is removed by improvement of the nominal model through the complementary phrase. Also, an improved frequency response obtained by fast Fourier transform (FFT) is clearly seen for the upgraded model (Fig. 3b).

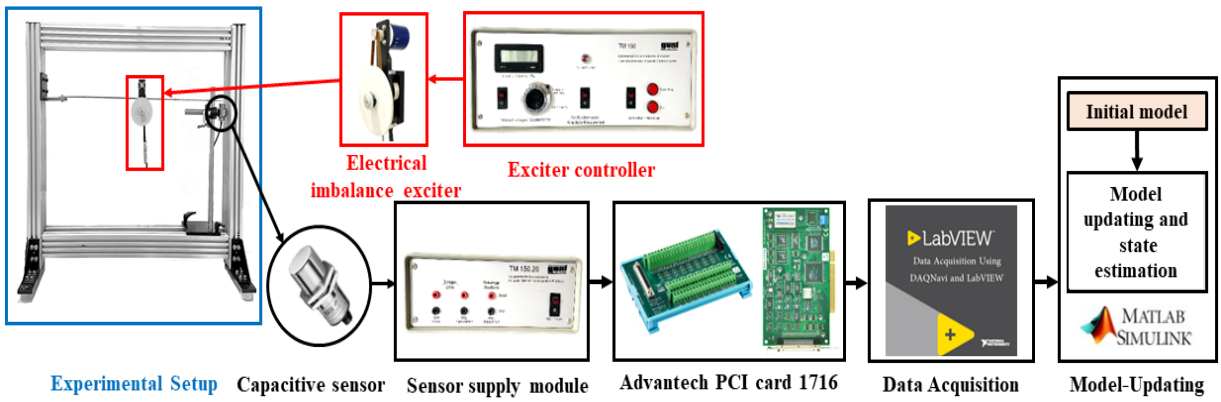

Figure 2 Experimental setup of the model-updating scheme

Table 1 The parameter of the flexible beam.

Parameter	Description	Value
L	Length of the beam	0.75 (m)
a	Height of the beam	0.004 (m)
b	Width of the beam	0.02 (m)
E	Young's modulus	207 (GPa)
ρ	Density	7801 (Kg/m^3)

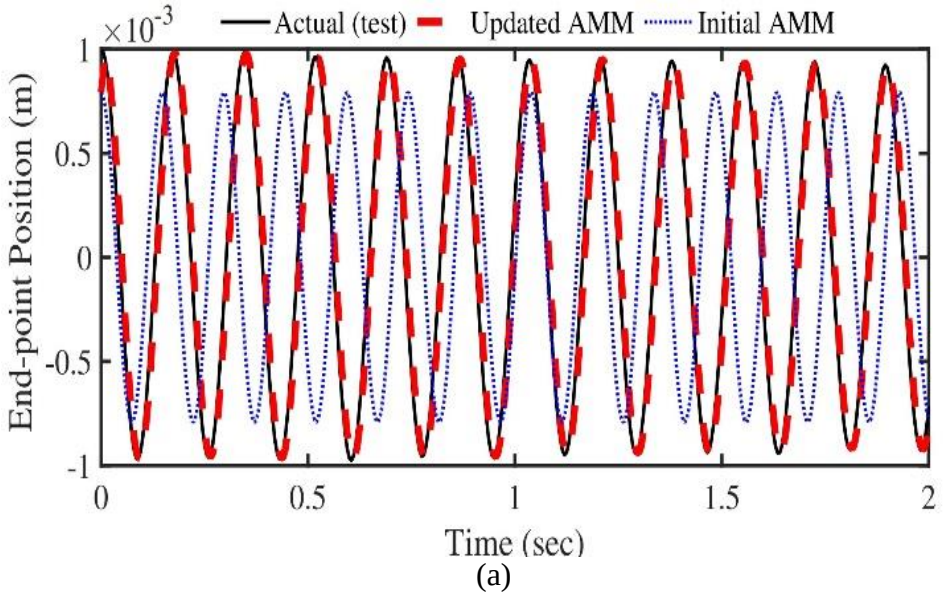

(a)

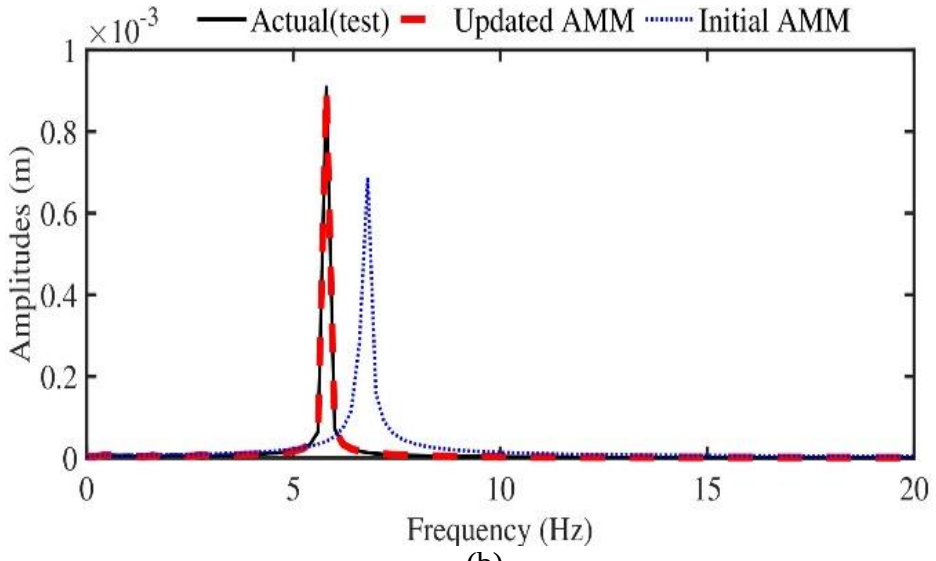

(b)

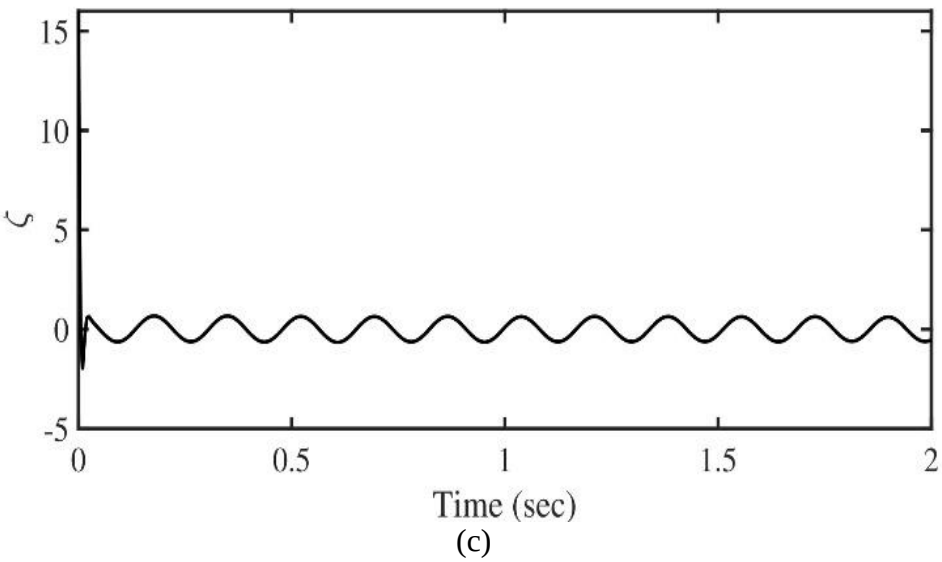

(c)

Figure 3 The experiment results in Case-1 during free vibration analysis, (**a**) End-point displacement, (**b**) FFT, (**c**) complementary phrase

4.1.2 Forced vibration

For analysis of the forced vibration under the suggested model-updating scheme, the beam of Case-2 is excited by the harmonic force with different frequencies. The force applied in the middle of the beam is modeled as $p_u = m_u r_u \omega^2 \sin(\omega t + \emptyset)$, for which $m_u = 0.01\ (kg)$ is the mass and $r_u = 0.01\ (m)$ is the eccentricity of exciter. Also, $\omega = 2$ and $4.2\ (Hz)$are selected as the excitation frequency. Note that, the disparity in the force-acting point is taken as the uncertainty.

Figures (4) and (5) present the system responses for forced vibrations. It is seen that the suggested estimation scheme can cope with the uncertainties, successfully. In the results, an increased amplitude is seen for the nominal model in Fig. (5). This increment is for the reason that the excitation frequency ($4.2\ (Hz)$) is close to the natural frequency of the actual beam found in Fig. (4). It is seen that for the harmonic excitation with the frequency of $4.2\ (Hz)$, the model-updating algorithm brings a phenomenon like beating in the complementary phrase to compensate for the uncertainties. This is for the reason that the excitation frequency is close to the natural frequency of the beam.

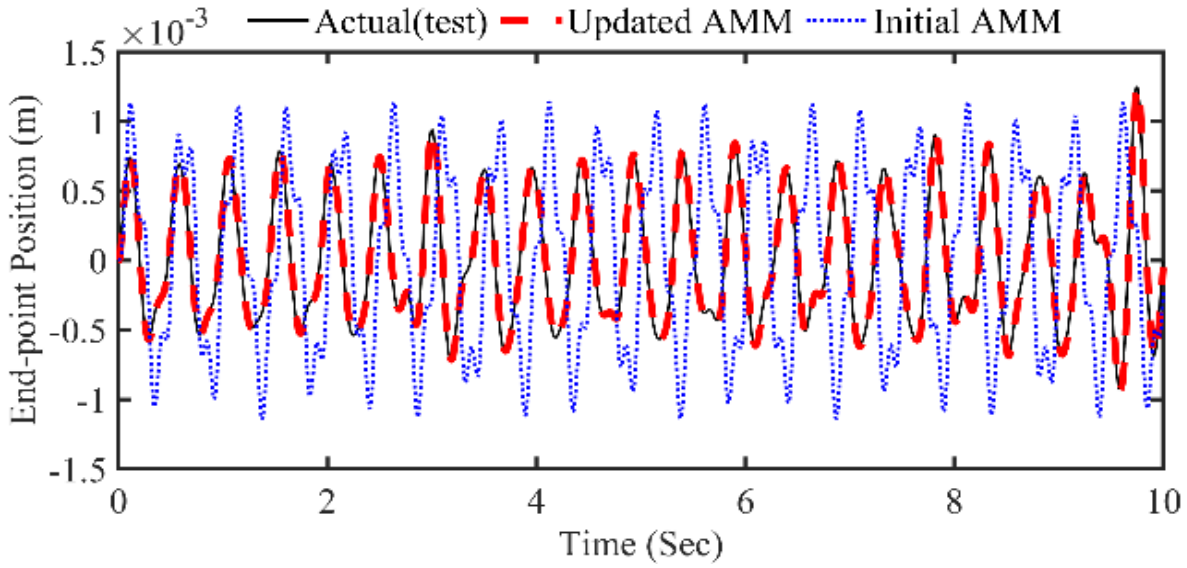

(a)

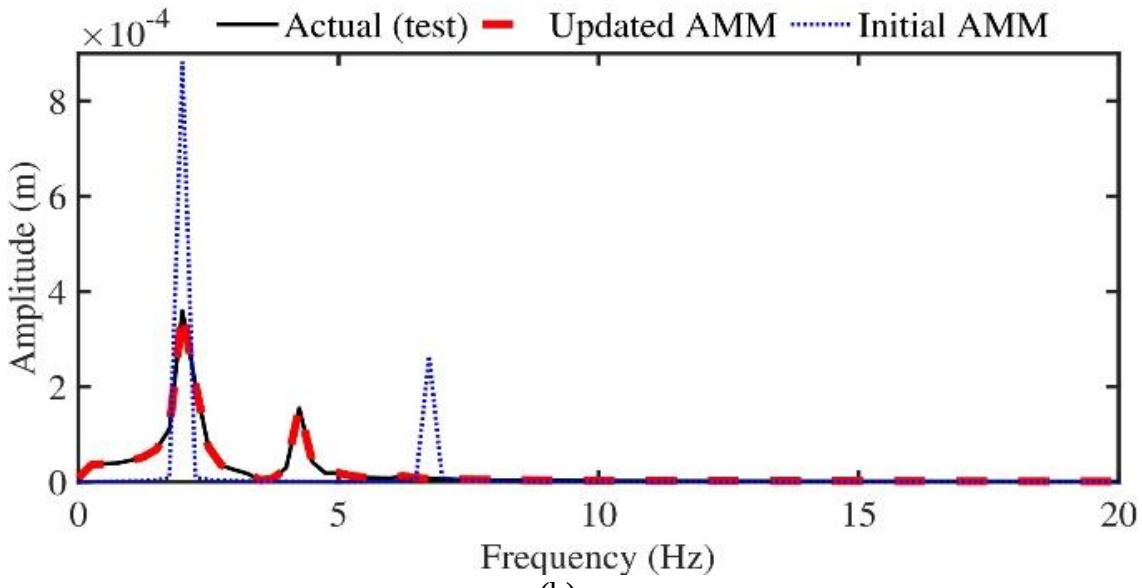

(b)

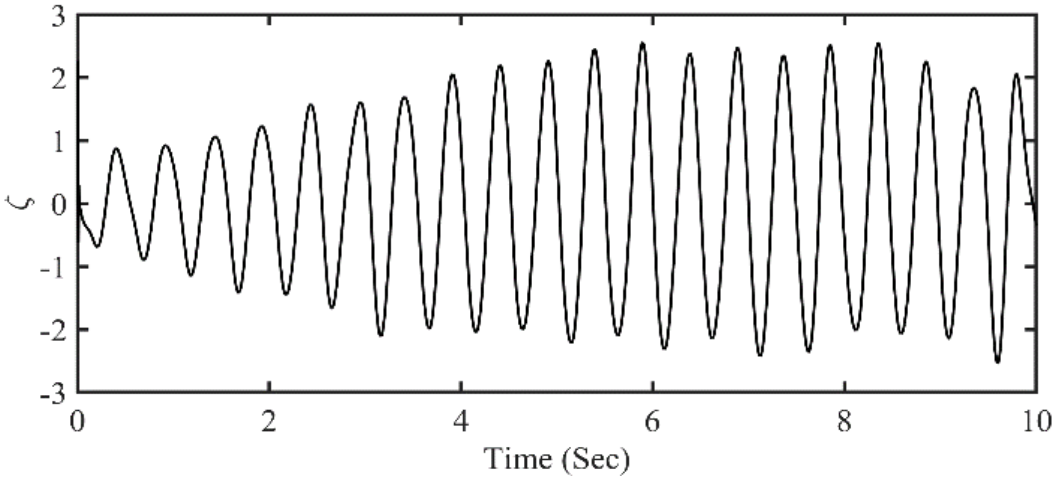

(c)

Figure 4 The experiment results in Case-2 with the excitation frequency of 2 (Hz), (**a**) End-point displacement, (**b**) FFT, (**c**) complementary phrase

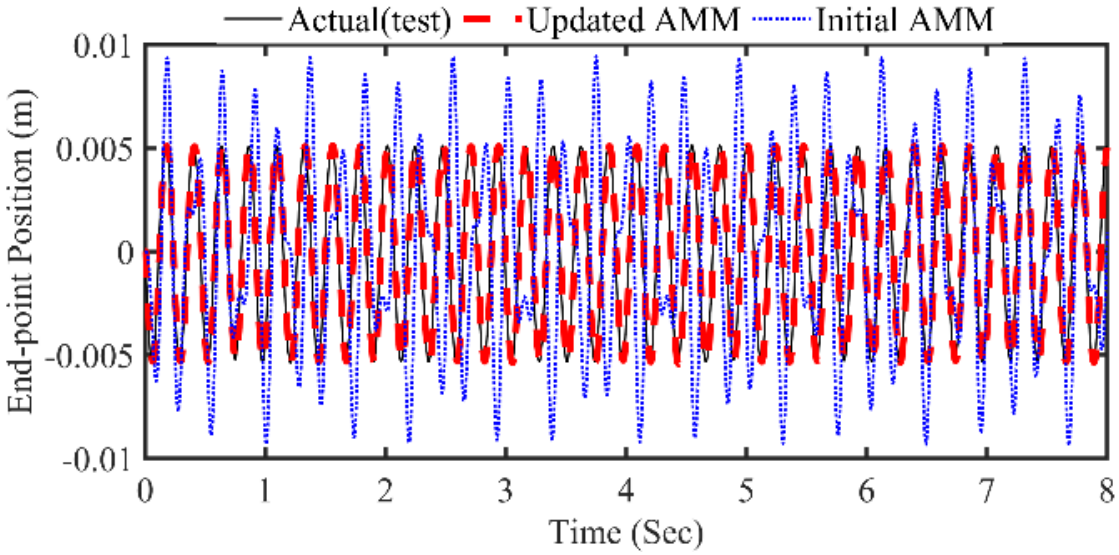

(a)

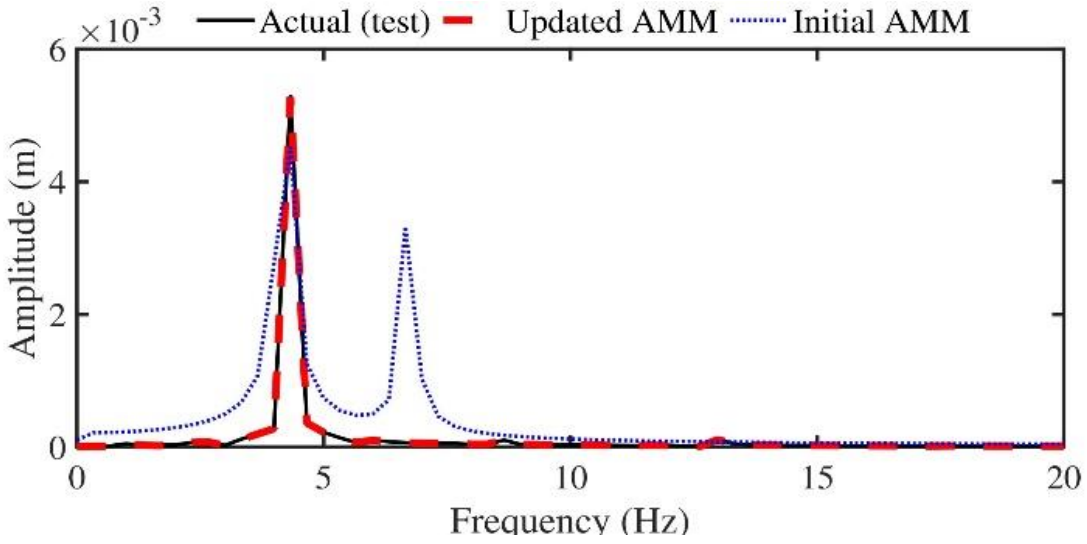

(b)

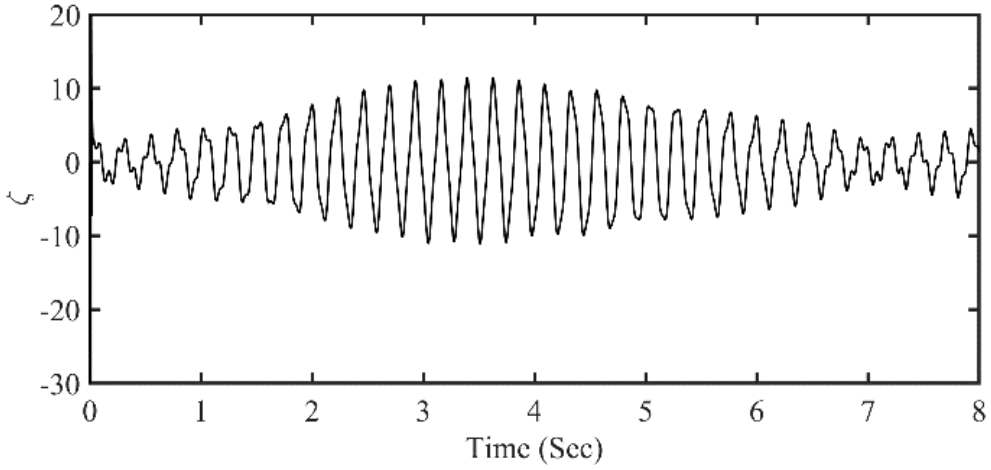

(c)

Figure 5 The experiment results in Case-2 with the excitation frequency of 4.2 (Hz), (**a**) End-point displacement, (**b**) FFT, (c) complementary phrase

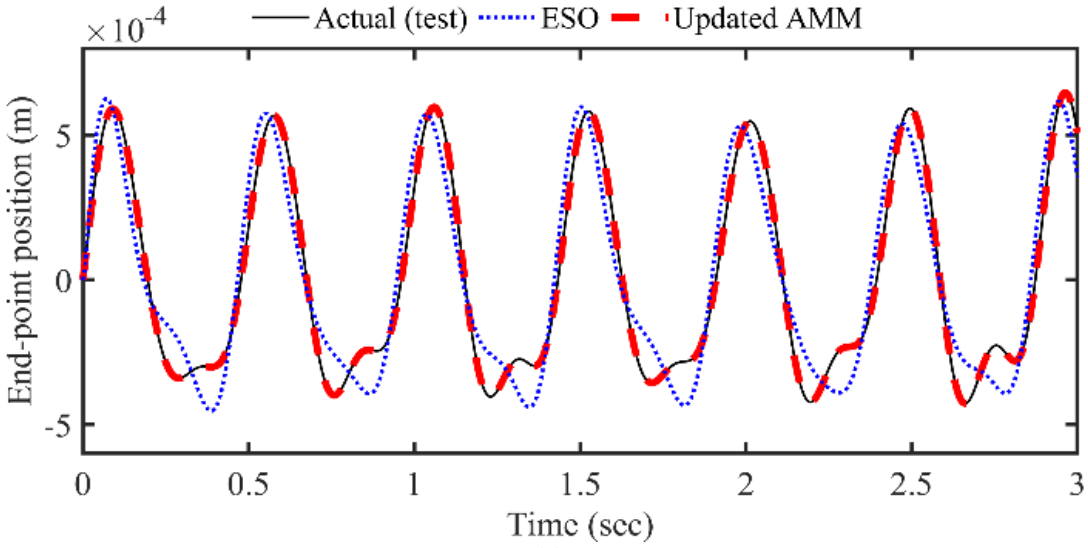

(a)

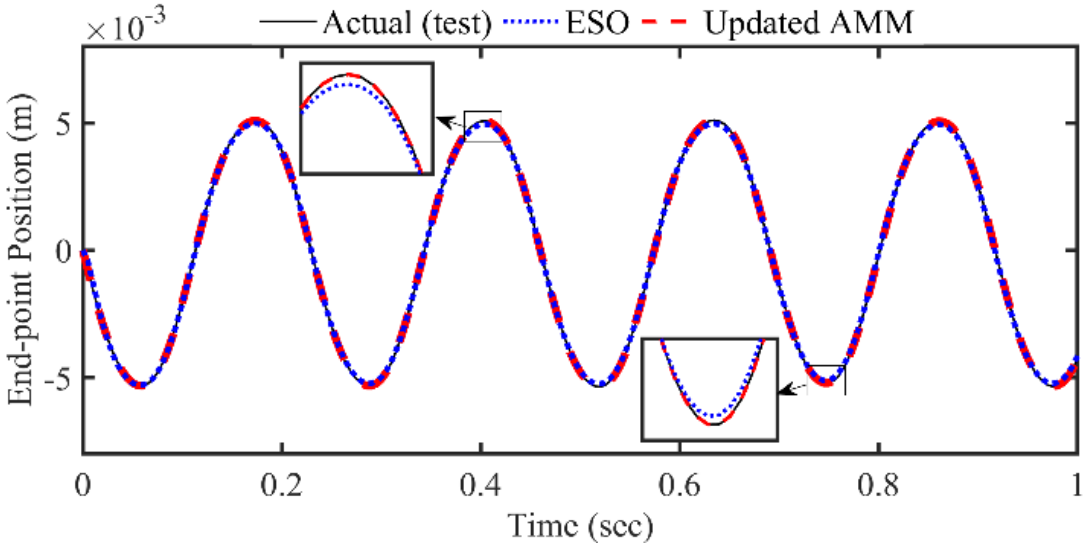

(b)

Figure 6 Proposed estimation method results for the forced vibration analysis in Case-2 in comparing with ESO, (**a**) End-point displacement in 2 (Hz) excitation, (**b**) End-point displacement in 4.2 (Hz) excitation

To compare the efficiency of the suggested model updating method with another uncertainty estimation strategy, the obtained results are compared with ESO. Both estimation methods use the same reduced-order model. According to Fig. (6), the suggested method is more efficient in reducing the estimation error compared to ESO. The estimation error in the suggested method converges to zero, whereas in ESO, as per Theorem 1, the estimation errors are bounded and will converge to a compact set.

4.2 Control system verification

The integration of the Adams and MATLAB software, presented in Fig. (7), is developed for examination of the suggested controller. The control signal is assumed to be a force applied at the beam's end-point to reduce free vibrations ($x_{1d} = 0$). The control signal should be calculated in the admissible range defined as $-10 \leq u \leq 10$ (N). In the Adams model, a flexible beam with parameters presented in Table (1) is designed, and a lumped mass is assumed to be at the middle of the beam. This mass is ignored in the nominal AMM-based model. Meanwhile, a parametric disparity of 40% in the Young's modulus is taken into account for the nominal model. According to Fig. (7), upgrading the nominal AMM-based model by the suggested scheme leads to a reliable model that is suitable for the design of the controller. The end-point displacement is extracted from the actual Adams model, and the control signal is transmitted to the Adams to constitute a software loop.
At first, the controller is examined by considering 2 (cm) initial end-point displacement. The results of the constrained control for three values of h are shown in Fig. (8). Given the smaller value of the prediction time $(h = 0.005)$, the control input in the unconstrained controller tends to take higher values. However, in the constrained controller, this results in more frequent saturation of the control input, which in turn degrades the system responses. This result is also confirmed by the outcome highlighted in Remark 4 for the constrained control. Consequently, it's advisable not to choose the prediction time too small. For the simulated feedback, $h = 0.01$ can be considered a reasonable choice. However, for larger values such as $h = 0.02$, the system response becomes slower, as noted in Remark 3.

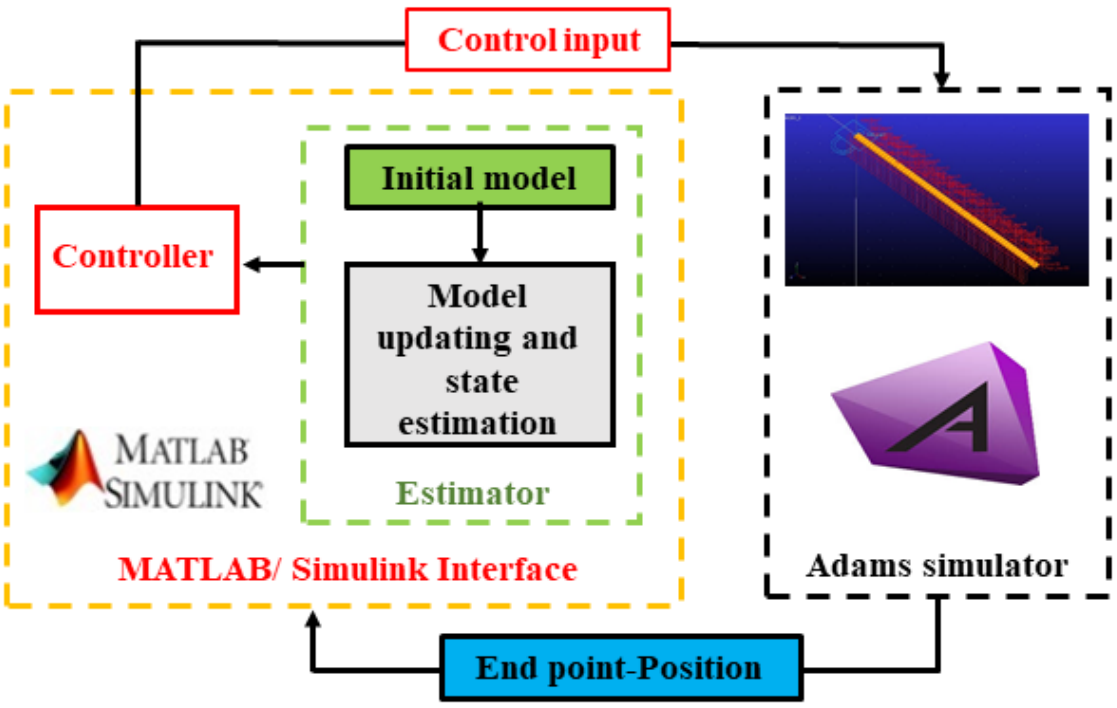

Figure 7 The software in the loop mechanization for the proposed control method

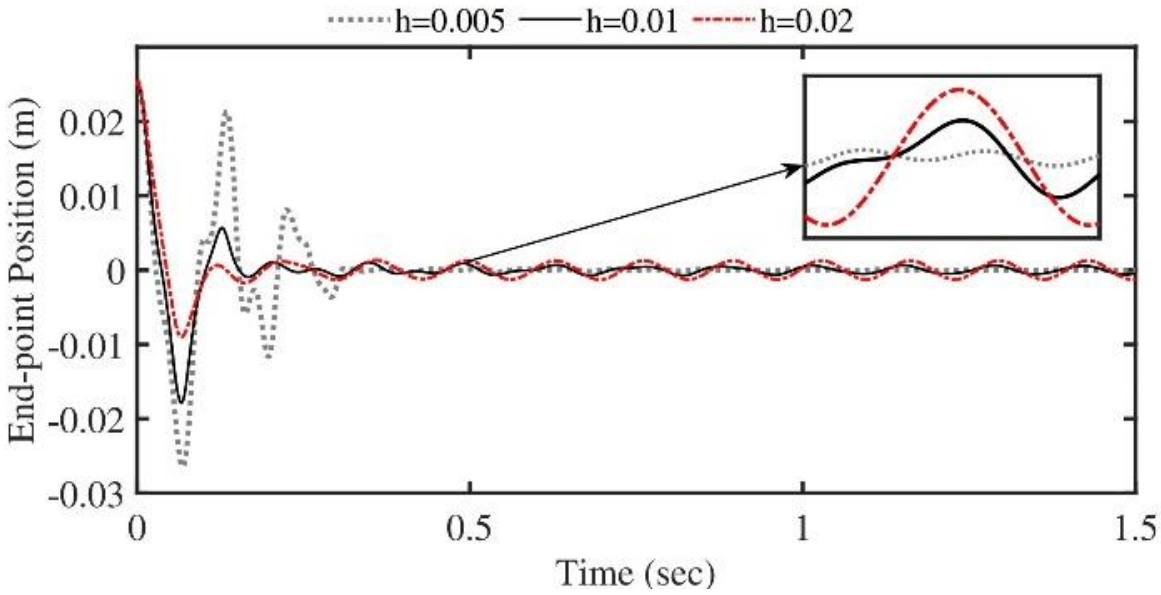

(a)

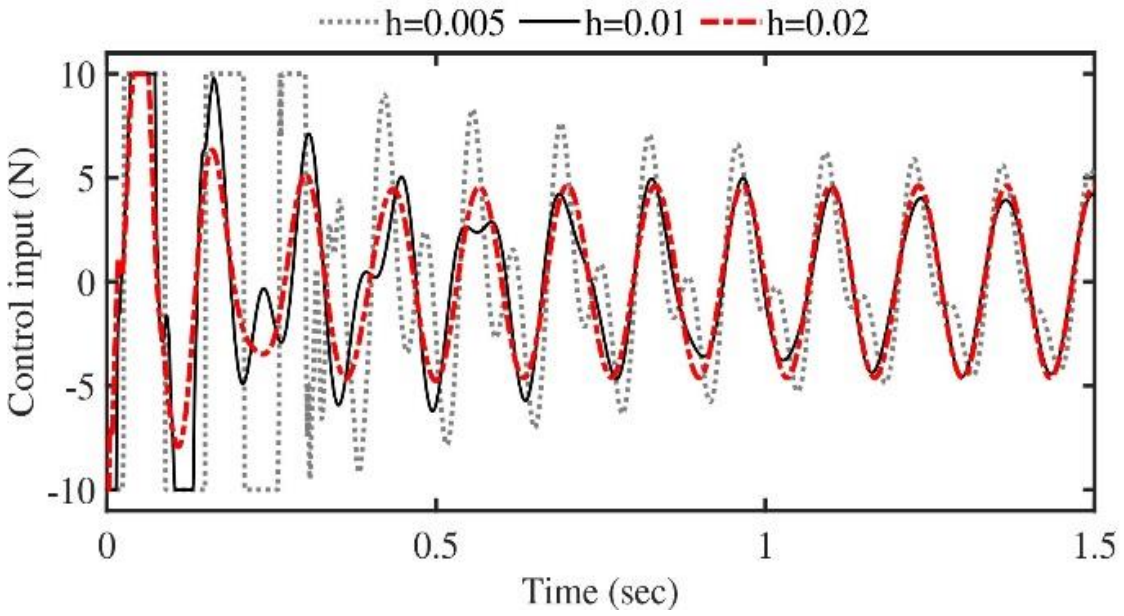

(b)

Figure 8 The result of the controlled beam in different prediction times for Case-2 with 2 (cm) initial end-point displacement, (**a**) End-point displacement, (**b**) Control force

The comparative response of the beam with and without control is depicted in Fig. (9). The complementary phrase is shown in Fig. (9c). The obtained results indicate that the controlled system leads to proper responses in suppression the vibration of the beam. Also, the estimator aims to enhance the reliability of the nominal AMM-based model by appending the complementary phrase. Consequently, the controller developed from the improved dynamic model exhibits great performance in mitigating the beam vibration.

In order to investigate the effect of updating the model through complementary phrase, the results are compared with the controller developed by the nominal AMM-based model without updating ($\xi = 0$). Figure (10) presents the comparative results for the $2\,(cm)$ initial displacement at the end-point of the beam. The results indicate that the vibration of the beam is remarkably reduced by the updated model-based controller compared with the controller without model updating, $\xi = 0$.

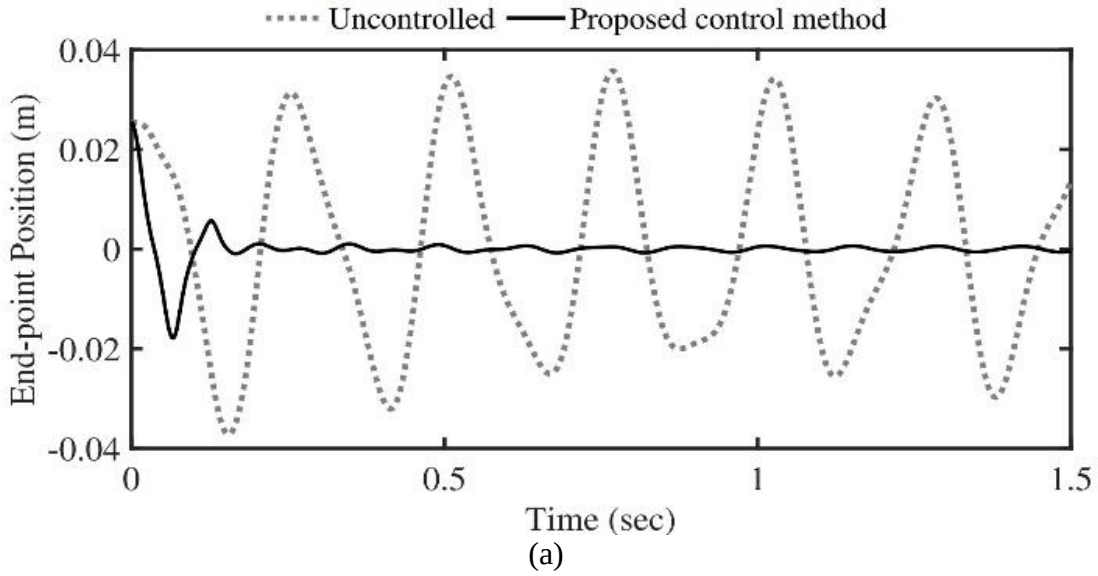

(a)

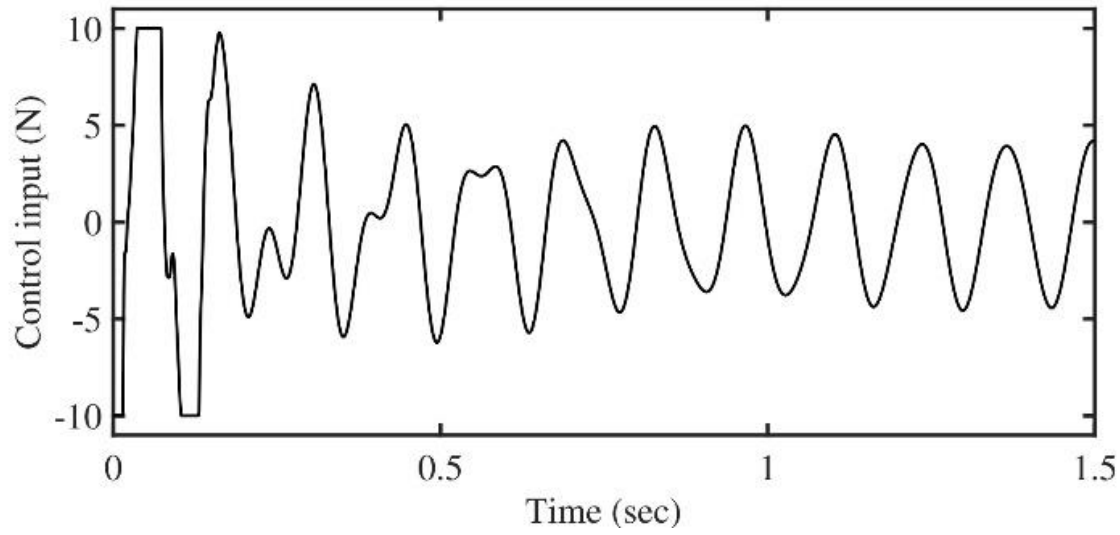

(b)

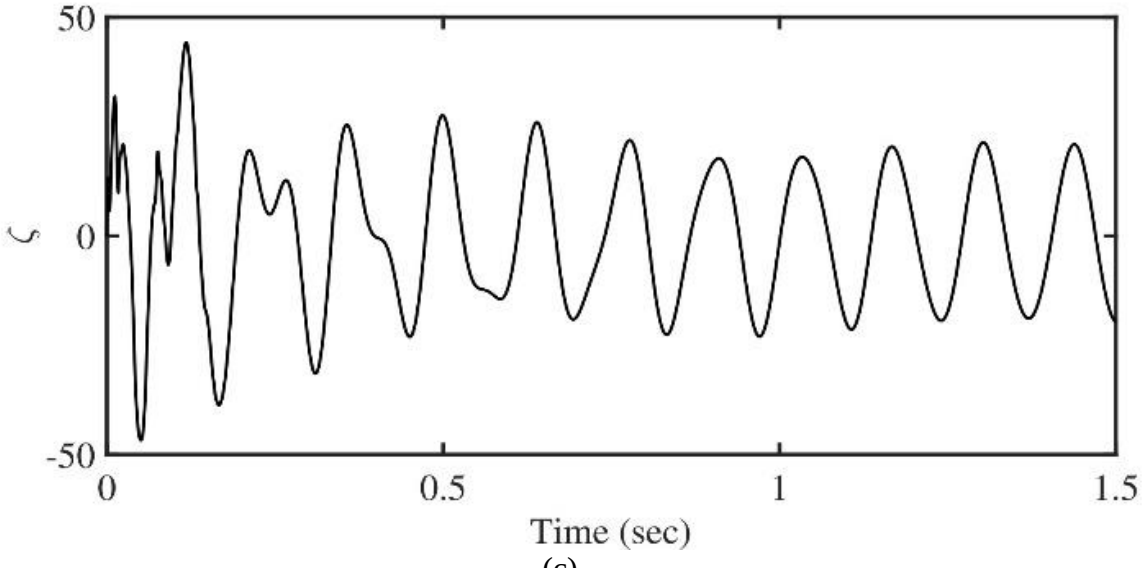

(c)

Figure 9 A comparative result of the controlled and uncontrolled beam in Case-2 with 2 (cm) initial end-point displacement, (**a**) End-point displacement, (**b**) Control force, (**c**) Complementary phrase

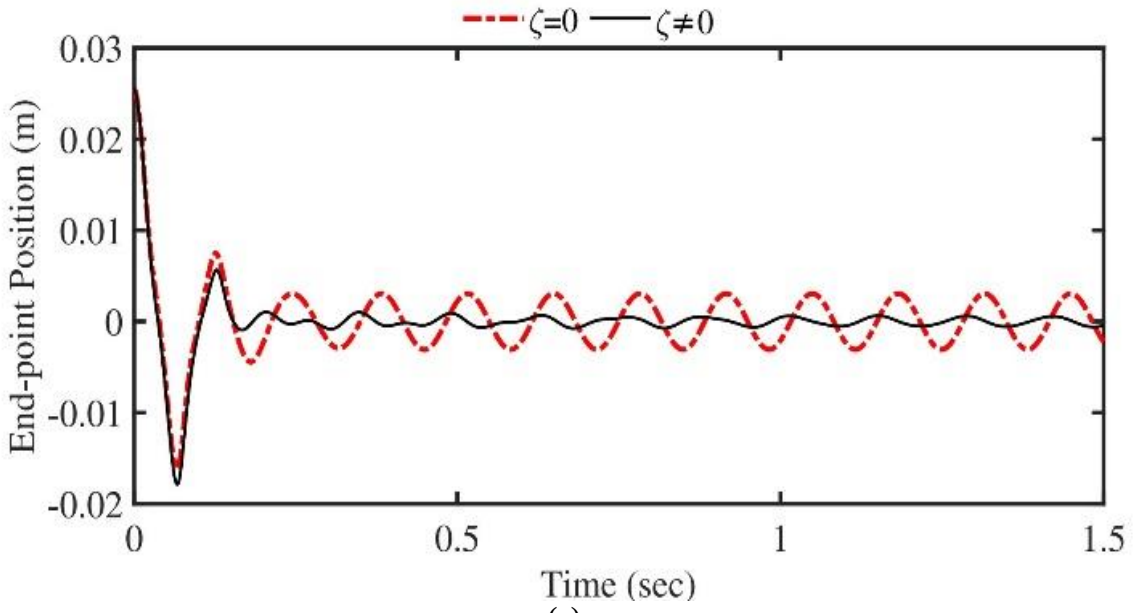

(a)

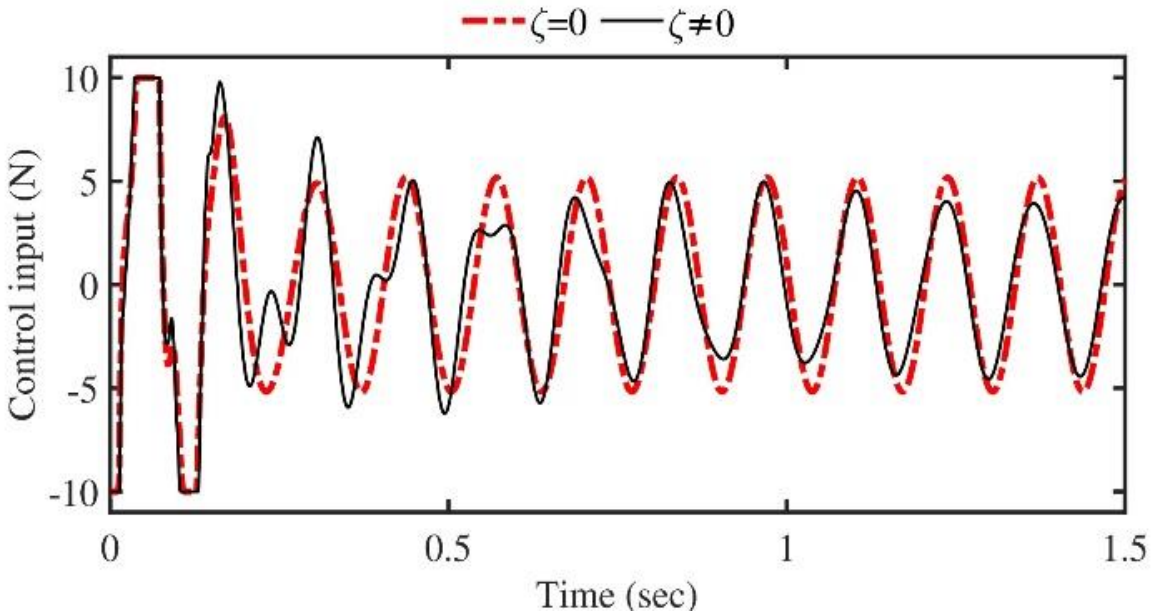

(b)

Figure 10 The results of the suggested control methods with and without model updating in Case-2 with 2 (cm) initial end-point displacement, (**a**) End-point displacement, (**b**) Control force

To assess the efficiency of the suggested constrained control scheme against other constrained strategies, the achieved outcomes are contrasted with those of conventional nonlinear model predictive control (NMPC) as described in Appendix (1). In this case, $5(cm)$ initial condition is considered at the end-point of the beam. Both methods utilize identical models and constraints for their implementation. As shown in Fig. (11), the efficiency of both approaches in satisfying the limitations are similar. However, the proposed control method with the updated model is more efficient in suppressing the beam vibrations in comparing with the NMPC. This is as a result of more saturations experienced by the NMPC due to the uncertainties. In addition, the suggested constrained controller is significantly faster than NMPC. The obtained results highlight the suitability of the proposed scheme for online implementation. It is important to note that, unlike the proposed algorithm, NMPC relies on online optimization at each instant to provide the control input.

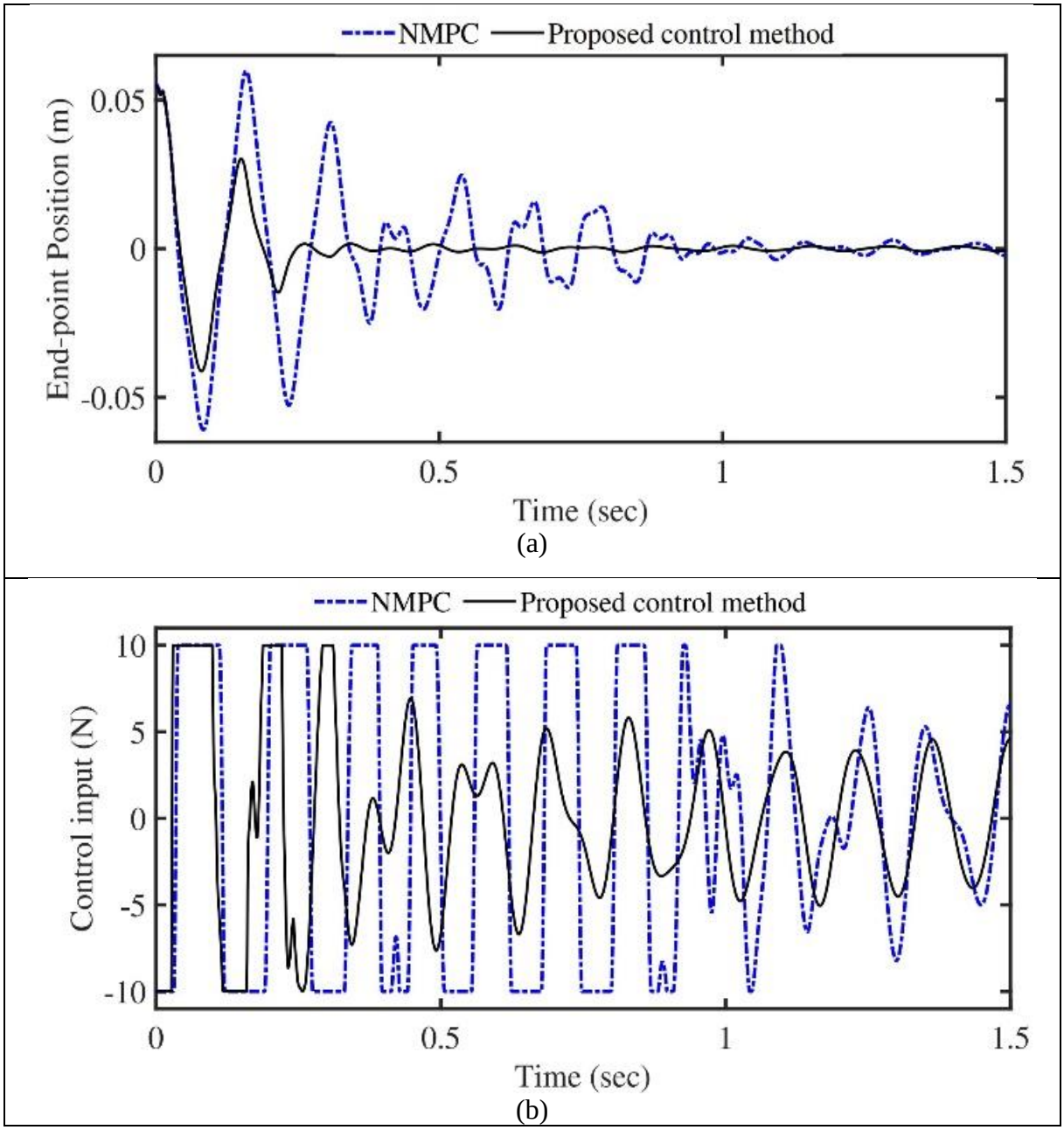

Figure 11 Comparison between the suggested control method and NMPC in Case-2 with 5 (cm) initial end-point displacement, (**a**) End-point displacement, **(b**) Control force

5 Conclusion

The discrepancy between the assumed mode model with the lowest DOF and the actual beam model is removed by estimating the model uncertainties. In this respect, a constrained control method according to the enriched model is developed to reduce vibrations of the beam. The stability of the proposed control method is analyzed to demonstrate the convergence of the errors.

Experimental tests are carried out for a flexible beam to demonstrate the high efficiency of the suggested model-updating scheme. Finally, the MATLAB-Adams co-simulation reveal that the proposed scheme leads to an accurate model in the presence of model perturbations. The resultant controller performs superiorly in suppressing the beam vibration. Additionally, the suggested control methods are compared with different control strategies. The results indicate that the suggested control method is significantly faster than NMPC.

References

[1] R. Mohsenipour, and G. Liu, "Flexible Single-link Manipulators Control Based on a Full-order Transfer Function Model," *IEEE Transactions on Automatic Control*, Vol. 69, No. 6, 2024, doi: https://doi.org/10.1109/TAC.2024.3351552.

[2] J. K. Viswanadhapalli, V. K. Elumalai, S. Shivram, S. Shah, and D. Mahajan, "Deep Reinforcement Learning with Reward Shaping for Tracking Control and Vibration Suppression of Flexible Link Manipulator," *Applied Soft Computing*, Vol. 152, pp. 110756, 2024, doi: https://doi.org/10.1016/j.asoc.2023.110756.

[3] Y. Wang, W. Wu, X. Lou, and D. Görges, "Iterative Learning Control of an Euler-Bernoulli Beam with Time-varying Boundary Disturbance," *Computers & Mathematics with Applications*, Vol. 162, pp. 145-154, 2024, doi: https://doi.org/10.1016/j.camwa.2024.03.004.

[4] E.-G. Liu, Y.-F. Shao, B. Dou, J.-F. Cui, and H. Ding, "High-order Modal Vibration Control of Timoshenko Beams Based on Nonlinear Energy Sink Cells," *Journal of Vibration Engineering & Technologies*, Vol. 12, pp. 6809-6819, 2024, doi: https://doi.org/10.1007/s42417-024-01284-5.

[5] Q. Yao, M. Luo, and D. Zhang, "Milling Dynamic Model Based on Rotatory Euler–Bernoulli Beam Model under Distributed Load," *Applied Mathematical Modelling*, Vol. 83, pp. 266-283, 2020, doi: https://doi.org/10.1016/j.apm.2020.02.015.

[6] X. Xing, and J. Liu, "PDE Modelling and Vibration Control of Overhead Crane Bridge with unknown Control Directions and Parametric Uncertainties," *IET Control Theory & Applications*, Vol. 14, No. 1, pp. 116-126, 2020, doi: https://doi.org/10.1007/978-981-16-1532-0_12.

[7] Y. Lei, T. Murmu, S. Adhikari, and M. Friswell, "Dynamic Characteristics of Damped Viscoelastic Nonlocal Euler–Bernoulli Beams," *European Journal of Mechanics-A/Solids*, Vol. 42, pp. 125-136, 2013, doi: https://doi.org/10.1016/j.euromechsol.2013.04.006.

[8] H. Wang, and G. Chen, "Asymptotic Locations of Eigenfrequencies of Euler–Bernoulli Beam with Nonhomogeneous Structural and Viscous Damping Coefficients," *SIAM Journal on Control and Optimization*, Vol. 29, No. 2, pp. 347-367, 1991, doi: https://doi.org/10.1137/0329019.

[9] I. Giorgio, and D. Del Vescovo, "Non-linear Lumped-parameter Modeling of Planar Multi-link Manipulators with Highly Flexible Arms," *Robotics*, Vol. 7, No. 4, pp. 60, 2018, doi: https://doi.org/10.3390/robotics7040060.

[10] K. Lochan, B. K. Roy, and B. Subudhi, "Robust Tip Trajectory Synchronisation between Assumed Modes Modelled Two-link Flexible Manipulators using Second-order PID Terminal SMC," *Robotics and Autonomous Systems*, Vol. 97, pp. 108-124, 2017, doi: https://doi.org/10.1016/j.robot.2017.08.008.

[11] R. Vidoni, L. Scalera, and A. Gasparetto, "3-D ERLS Based Dynamic Formulation for Flexible-link Robots: Theoretical and Numerical Comparison between the Finite Element Method and the Component Mode Synthesis Approaches," *International Journal of Mechanics*

and Control, Vol 19, No 1, pp. 39-50, 2018. [Online]. Available: https://bia.unibz.it/esploro/outputs/991005772712201241.

[12] S. Grazioso, V. Sonneville, G. Di Gironimo, O. Bauchau, and B. Siciliano, "A Nonlinear Finite Element Formalism for Modelling Flexible and Soft Manipulators," in *2016 IEEE International Conference on Simulation, Modeling, and Programming for Autonomous Robots (SIMPAR)*, 13-16 December 2016: IEEE, San Francisco, CA, USA, pp. 185-190, doi: https://doi.org/10.1109/SIMPAR.2016.7862394.

[13] N. Mishra, and S. Singh, "Determination of Modes of Vibration for Accurate Modelling of the Flexibility Effects on Dynamics of a Two Link Flexible Manipulator," *International Journal of Non-linear Mechanics*, Vol. 141, pp. 103943, 2022, doi: https://doi.org/10.1016/j.ijnonlinmec.2022.103943.

[14] M. O. Tokhi, and A. K. Azad, "*Flexible Robot Manipulators: Modelling, Simulation and Control"*, First Edition, Institution of Engineering and Technology-IET, London, United Kingdom, 2008, ISBN:9780863414480, 0863414486, doi: https://doi.org/10.1049/PBCE068E.

[15] J. Fan, D. Zhang, and H. Shen, "Dynamic Modeling and Simulation of a Rotating Flexible Hub-beam Based on Different Discretization Methods of Deformation Fields," *Archive of Applied Mechanics*, Vol. 90, pp. 291-304, 2020, doi: https://doi.org/10.1007/s00419-019-01609-x.

[16] H. H. Yoo, J. E. Cho, and J. Chung, "Modal Analysis and Shape Optimization of Rotating Cantilever Beams," *Journal of Sound and Vibration*, Vol. 290, No. 1-2, pp. 223-241, 2006, doi: https://doi.org/10.1016/j.jsv.2005.03.014.

[17] M. Raoufi, and H. Delavari, "Experimental Implementation of a Novel Model-free Adaptive Fractional-order Sliding Mode Controller for a Flexible-link Manipulator," *International Journal of Adaptive Control and Signal Processing*, Vol. 35, No. 10, pp. 1990-2006, 2021, doi: https://doi.org/10.1002/acs.3305.

[18] A. Green, and J. Sasiadek, "Robot Manipulator Control for Rigid and Assumed Mode Fexible Dynamics Models," in *AIAA Guidance, Navigation, and Control Conference and Exhibit*, 11-14 August, 2003, Autin, Texas, pp. 5435, doi: https://doi.org/10.2514/6.2003-5435.

[19] T. Bhaskarwar, H. F. Hawari, N. B. Nor, R. H. Chile, D. Waghmare, and S. Aole, "Sliding Mode Controller with Generalized Extended State Observer for Single Link Flexible Manipulator," *Applied Sciences*, Vol. 12, No. 6, pp. 3079, 2022, doi: https://doi.org/10.3390/app12063079.

[20] R. M. Gharamaleki, M. Mirzaei, S. Rafatnia, and B. Alizadeh, "An Analytical Approach to Optimal Control of Nonlinear Systems with Input Constraints," *International Journal of Automation and Control*, Vol. 14, No. 2, pp. 213-238, 2020, doi: https://doi.org/10.1504/IJAAC.2020.105519.

[21] A. Ghiasi, G. Alizadeh, and M. Mirzaei, "Simultaneous Design of Optimal Gait Pattern and Controller for a Bipedal Robot," *Multibody System Dynamics*, Vol. 23, pp. 401-429, 2010, doi: https://doi.org/10.1007/s11044-009-9185-z.

[22] A. Tahouni, M. Mirzaei, and B. Najjari, "Applied Nonlinear Control of Vehicle Stability with Control and State Constraints," *Proceedings of the Institution of Mechanical Engineers, Part D: Journal of Automobile Engineering*, Vol. 234, No. 1, pp. 191-211, 2020, doi: https://doi.org/10.1177/0954407019848858.

[23] R. Azmi, M. Mirzaei, and A. Habibzadeh-Sharif, "A Novel Optimal Control Strategy for Regenerative Active Suspension System to Enhance Energy Harvesting," *Energy Conversion and Management*, Vol. 291, pp. 117277, 2023, doi: https://doi.org/10.1016/j.enconman.2023.117277.

[24] J. Li, L. Zhang, L. Luo, and S. Li, "Extended State Observer Based Current-constrained Controller for a PMSM System in Presence of Disturbances: Design, Analysis and Experiments," *Control Engineering Practice*, Vol. 132, pp. 105412, 2023, doi: https://doi.org/10.1016/j.conengprac.2022.105412.

[25] F. Pak, M. Mirzaei, S. Rafatnia, and S. Salmani Pour Avval, "Novel Observer-based Input-constrained Control of Nonlinear Second-order Systems with Stability Analysis: Experiment on Lever Arm," *Iranian Journal of Science and Technology, Transactions of Electrical Engineering*, pp. 1-18, 2024, doi: https://doi.org/10.1007/s40998-024-00713-1.

[26] B.-Z. Guo, and Z.-l. Zhao, "On the Convergence of an Extended State Observer for Nonlinear Systems with Uncertainty," *Systems & Control Letters*, Vol. 60, No. 6, pp. 420-430, 2011, doi: https://doi.org/10.1016/j.sysconle.2011.03.008.

[27] M. M. Shahir, M. Mirzaei, M. Farbodi, and S. Rafatnia, "Extended State Observer-Based Feedback Linearization Control of Shape Memory Alloy Actuator: Design and Experiment," *International Journal of Dynamics and Control*, pp. 1-12, 2023, doi: https://doi.org/10.1007/s40435-023-01362-8.

[28] H. Gui, L. Jin, and S. Xu, "Simple Finite-Time Attitude Stabilization Laws for Rigid Spacecraft with Bounded Inputs," *Aerospace Science and Technology*, Vol. 42, pp. 176-186, 2015, doi: https://doi.org/10.1016/j.ast.2015.01.020.

[29] A. M. Zou, A. H. de Ruiter, and K. D. Kumar, "Finite-Time Attitude Tracking Control for Rigid Spacecraft with Control Input Constraints," *IET Control Theory & Applications*, Vol. 11, No. 7, pp. 931-940, 2017, doi: https://doi.org/10.1049/iet-cta.2016.1097.

[30] J.-H. Tsai, Y.-Y. Du, W.-Z. Zhuang, S.-M. Guo, C.-W. Chen, and L.-S. Shieh, "Optimal Anti-Windup Digital Redesign of Multi-Input Multi-Output Control Systems under Input Constraints," *IET Control Theory & Applications*, Vol. 5, No. 3, pp. 447-464, 2011, doi: https://doi.org/0.1049/iet-cta.2010.0020.

[31] Y. Su, and J. Swevers, "Finite-time Tracking Control for Robot Manipulators with Actuator Saturation," *Robotics and Computer-integrated Manufacturing*, Vol. 30, No. 2, pp. 91-98, 2014, doi: https://doi.org/10.1016/j.rcim.2013.09.005.

[32] Z. Ma, and P. Huang, "Adaptive Neural-network Controller for an Uncertain Rigid Manipulator with Input Saturation and Full-order State Constraint," *IEEE Transactions on Cybernetics*, Vol. 52, No. 5, pp. 2907-2915, 2020, doi: https://doi.org/10.1109/TCYB.2020.3022084.

[33] D. E. Kirk, "*Optimal Control Theory: An Introduction*", First Publication, Courier Corporations, Dover Publications, Inc., Mineola, New York, 2004, doi: https://doi.org/10.1002/aic.690170452.

[34] R. C. Loxton, K. L. Teo, V. Rehbock, and K. F. C. Yiu, "Optimal Control Problems with a Continuous Inequality Constraint on the State and the Control," *Automatica*, Vol. 45, No. 10, pp. 2250-2257, 2009, doi: https://doi.org/10.1016/j.automatica.2009.05.029.

[35] H. Marzban, and M. Razzaghi, "Rationalized Haar Approach for Nonlinear Constrained Optimal Control Problems," *Applied Mathematical Modelling*, Vol. 34, No. 1, pp. 174-183, 2010, doi: https://doi.org/10.1016/j.apm.2009.03.036.

[36] D. Liu, D. Wang, and X. Yang, "An Iterative Adaptive Dynamic Programming Algorithm for Optimal Control of unknown Discrete-time Nonlinear Systems with Constrained Inputs," *Information Sciences*, Vol. 220, pp. 331-342, 2013, doi: https://doi.org/10.1016/j.ins.2012.07.006.

[37] S. Mashayekhi, Y. Ordokhani, and M. Razzaghi, "Hybrid Functions Approach for Nonlinear Constrained Optimal Control Problems," *Communications in Nonlinear Science and Numerical Simulation*, Vol. 17, No. 4, pp. 1831-1843, 2012, doi: https://doi.org/10.1016/j.cnsns.2011.09.008.

[38] D.-P. Li, D.-J. Li, Y.-J. Liu, S. Tong, and C. P. Chen, "Approximation-based Adaptive Neural Tracking Control of Nonlinear MIMO unknown Time-varying Delay Systems with Full State Constraints," *IEEE Transactions on Cybernetics*, Vol. 47, No. 10, pp. 3100-3109, 2017, doi: https://doi.org/10.1109/TCYB.2017.2707178.

[39] Z. Chen, Z. Li, and C. P. Chen, "Adaptive Neural Control of Uncertain MIMO Nonlinear Systems with State and Input Constraints," *IEEE Transactions on Neural Networks and Learning Systems*, Vol. 28, No. 6, pp. 1318-1330, 2016, doi: https://doi.org/10.1109/TNNLS.2016.2538779.

[40] C. E. Garcia, D. M. Prett, and M. Morari, "Model Predictive Control: Theory and Practice—A Survey," *Automatica*, Vol. 25, No. 3, pp. 335-348, 1989, doi: https://doi.org/10.1016/0005-1098(89)90002-2.

[41] N. F. Silva Jr, C. E. T. Dórea, and A. L. Maitelli, "An Iterative Model Predictive Control Algorithm for Constrained Nonlinear Systems," *Asian Journal of Control*, Vol. 21, No. 5, pp. 2193-2207, 2019, doi: https://doi.org/10.1002/asjc.1815.

[42] S. S. Rao, "*Vibration of Continuous Systems*", John Wiley & Sons, United Kingdom, 2019, ISBN:9781119424147, 1119424143 , doi: https://doi.org/ 10.1002/9780470117866.

[43] Z. A. Sisi, M. Mirzaei, and S. Rafatnia, "Estimation of Vehicle Suspension Dynamics with Data Fusion for Correcting Measurement Errors," *Measurement*, Vol. 231, pp. 114438, 2024, doi: https://doi.org/10.1016/j.measurement.2024.114438.

[44] S. Rafatnia, and M. Mirzaei, "Estimation of Reliable Vehicle Dynamic Model using IMU/GNSS Data Fusion for Stability Controller Design," *Mechanical Systems and Signal Processing*, Vol. 168, pp. 108593, 2022, doi: https://doi.org/10.1016/j.ymssp.2021.108593.

[45] C.-T. Chen, "*Linear System Theory and Design"*, Saunders College Publishing, Oxford University Press Inc., New York, NY, United States, 1998, [Online] Available: https://dl.acm.org/doi/10.5555/521603.

[46] S. Jamshidi, M. Mirzaei, and M. Malekzadeh, "Applied Nonlinear Control of Spacecraft Simulator with Constraints on Torque and Momentum of Reaction Wheels," *ISA Transactions*, Vol. 138, pp. 705-719, 2023, doi: https://doi.org/10.1016/j.isatra.2023.03.027.

[47] B. Najjari, M. Mirzaei, and A. Tahouni, "Decentralized Integration of Constrained Active Steering and Torque Vectoring Systems to Energy-efficient Stability Control of Electric Vehicles," *Journal of the Franklin Institute*, Vol. 359, No. 16, pp. 8713-8741, 2022, doi: https://doi.org/10.1016/j.jfranklin.2022.08.035.

[48] S. K. Samiei, M. Mirzaei, and S. Rafatnia, "Constrained Control of Flexible-joint Lever Arm Based on Uncertainty Estimation with Data Fusion for Correcting Measurement Errors," *Nonlinear Dynamics*, pp. 1-20, 2024, doi: https://doi.org/10.1007/s11071-024-09637-1.

[49] S. J. Wright, "*Numerical Optimization"*, Springer-Verlag New York, Inc., New York, NY, United States, 2006, doi: https://doi.org/10.1007/978-0-387-40065-5.

[50] H. K. Khalil, "*Control of Nonlinear Systems*", Prentice Hall, New York, NY, United States, 2002, Available: https://books.google.com/books/about/Nonlinear_Control.html?id=-WbjoAEACAAJ.

Appendix 1: Nonlinear Model Predictive Control Scheme

Nonlinear Model Predictive Control (NMPC) is a powerful and widely used method for constrained control of nonlinear systems. To evaluate the efficiency of the suggested control method for the flexible beam, we compare its results with those achieved by a constrained NMPC approach. Figure (12) illustrates the structure of the constrained NMPC algorithm. The NMPC algorithm, as shown in Fig. (12), consists of three main blocks: a prediction block to predict future system states, a cost function block to define the optimization objective, and a minimization block to find the control input that minimizes the cost while respecting constraints. The discrete model of beam is used in this algorithm. As shown in Fig. (13), both the control horizon and the prediction horizon are set to 5 and 10 steps, respectively. Consequently, when $k = 0$, the control horizon will be from $k = 0$ to $k = 0$ and the predictive horizon will be from $k = 1$ to $k = 10$.

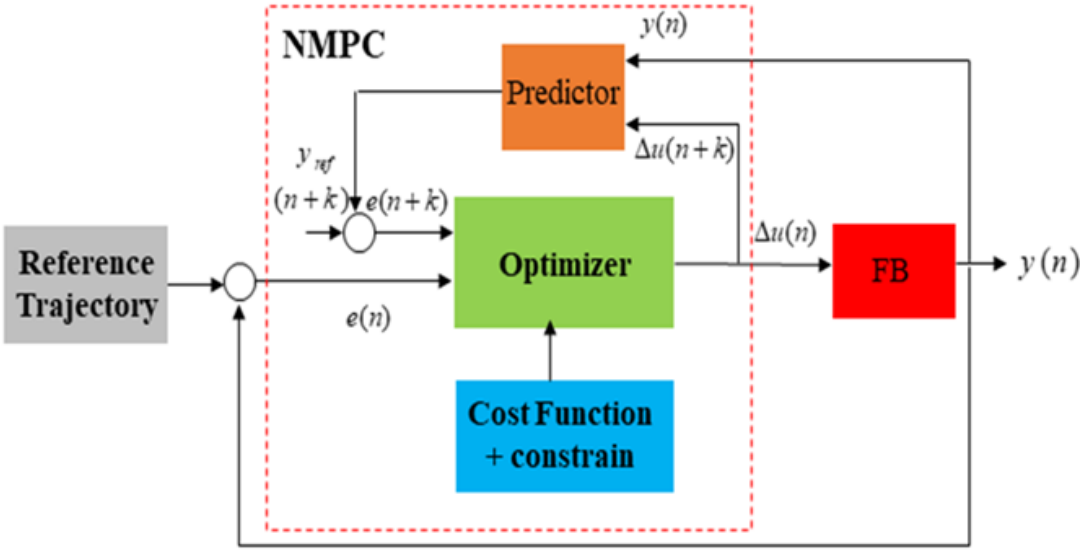

Figure 12 NMPC algorithm for a FB

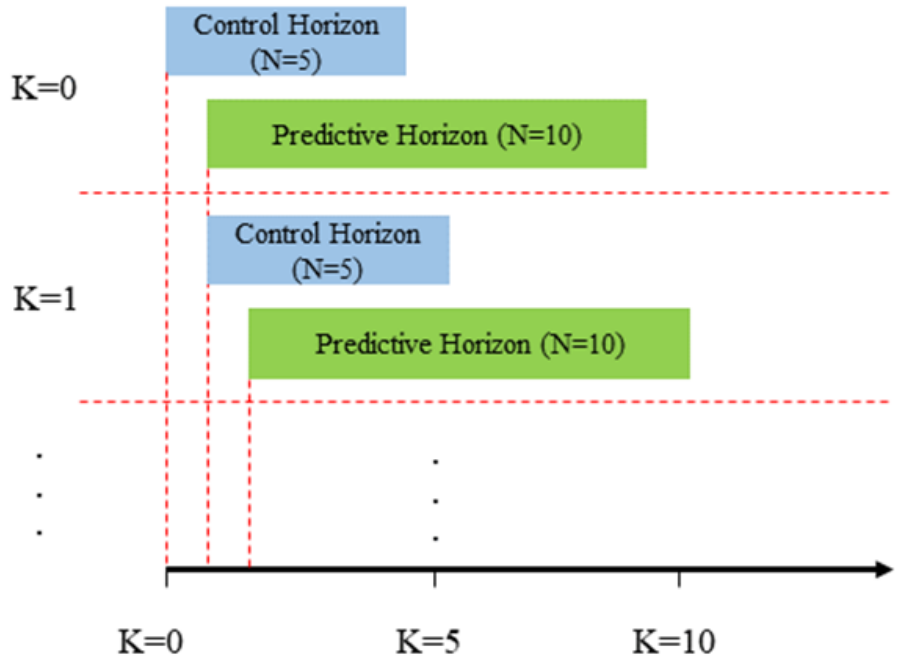

Figure 13 A discrete NMPC approach